

The authors would like to thank the editor for the detailed comments and for taking the time to carefully read our revision and our reply to the referees.

We believe there are a few aspects that might have been misinterpreted, especially regarding the nature and properties of the methods applied in the study. This is not surprising, as the methods applied here based on “machine learning” represent a new statistical model paradigm that differs from the commonly used linear regression based modelling of land surface phenology (LSP). LSP has previously been modelled using traditional linear regression approaches in most of the studies in the literature. However, this is not the case in our study, as we have used an innovative machine learning technique called Random Forest. This has important implications for understanding of our results and it makes an interpretation in a similar way as classical linear multiple regression inappropriate.

There are different aspects that make machine learning techniques, such as Random Forest, substantially different to linear regression:

- i. There are no formal distribution assumptions (non-parametric);
- ii. It can learn complex patterns, taking into account any nonlinear complex relationship between the predictor and the dependent variables (non-linearity);
- iii. It can handle thousands of predictors without variable deletion (no need for independency between explanatory variables).

We believe that the methodology proposed here is new and sound, but more importantly this study offers new insights into the modelling and our understanding of LSP, avoiding some of the limitations of multiple linear regressions.

A detailed response to editor comments is given below:

Comment 1: “I was missing the critical discussion of the implicit assumption that one single model should be able to describe phenology across an entire continent, i.e. comprising different species and climates and ecological factors. That phenology at different locations and in differing species is driven by different drivers in differing ways is at least more likely.”

Reply 1: We agree with the editor that having a model for the entire Europe would not be very realistic and will not capture the contribution of key drivers. However, this is not our case. Rather than having one single global model for the entire Europe, we have built multiple individual models (2000) from different data subsets and using different explanatory variables (climatic predictors). This is why the approach is termed as ‘Random Forest’. The estimates of all those models are taken into account to predict the LSP at a given location and time. Therefore, different drivers for different biogeographical areas are implicitly considered.

To understand our modelling approach it is important to know how the Random Forest algorithm works. We believe that we might have failed in giving a comprehensive explanation of the method. Therefore, we have made an effort to improve the description of the methodology, rewriting section 3.4, adding a new figure, and improving figure captions. Section 3.4 has been rewritten as follows:

“Conventional statistical models such as linear regression might be inappropriate for investigating the drivers of interannual variation in phenology because many of the relationships are likely to be non-linear (De Beurs and Henebry, 2008). In this sense, machine learning methods have emerged as complementary alternatives to conventional statistical techniques. Within the branch of machine learning techniques, regression trees are particularly suitable when compared to global single predictive models, allowing for multiple regression models using recursive partitioning (Breiman et al., 1984). Assembling a single global model might not be representative of LSP of the entire European continent, when there are many climatic drivers which interact in complicated, non-linear ways and may vary spatially and temporally. For the purpose of this paper, an alternative approach is to sub-divide, or partition, the data space into more homogeneous regions of similar climates and ecological factors.

Regression trees use a sum of squares criterion to split the data into successively more homogeneous subsets contained at many different structural units called nodes. Each of the terminal nodes, has attached to it a simple regression which applies in that node only. Therefore, different regressions can be fitted to different data subsets within one single regression tree, which can represent different responses controlled by different drivers (Archibald et al., 2009; Lawler et al., 2006). Additionally, the performance of multiple regression trees can be combined to increase the predictive ability of a single regression tree model, following the Random Forest technique (Figure 3). The RF method is an innovative machine learning approach that can perform multivariate non-linear regression, combining the performance of numerous regression tree algorithms to predict the interannual variation in OG and EOS. More details regarding the performance and the specific characteristics of a RF model can be seen in Rodriguez-Galiano et al. (2015b); Rodriguez-Galiano et al. (2014), and Figure 3..

The Random Forest method was applied to phenological modelling across very large areas and across multiple years simultaneously: the typical case for satellite-observed LSP. The RF model was fitted to the relation between LSP interannual variation and numerous climate predictor variables computed at biologically-relevant rather than human-imposed temporal scales. We restricted our climate data choices to daily data (average, minimum and maximum temperatures, precipitation and radiation) to account for integrative forcing (that is, growing degree days, chilling requirements as well as cumulative precipitation and radiation), computed from the exact day of the phenological event backwards, rather than using the calendar months. The locations with z-score in LSP greater than 1 (positive and negative) were selected to build a RF predictive model on OG and EOS. Z-score values of OG or EOS for each year were combined together with the different weather predictors. The z-score values in OG were

assessed as an extra predictor to evaluate the legacy effect of an advanced or delayed spring in the modelling of EOS. The values of these variables at the selected years and locations (spatiotemporal model) were combined into a set of input feature vectors (3900 feature vectors for the spring model and 3124 for autumn) as an input to the RF algorithm. These feature vectors were divided equally into two subsets, one for the training of the models (inbag) and one as an additional test to the one internally computed by RF (out of bag; oob) to evaluate performance. RF models composed of 2000 trees were grown using different subsets of predictors, varying the number of random predictors from 1 to 9. The Random Forest method within the package implemented in the R statistical software was used to build the different models (Liaw and Wiener, 2002).

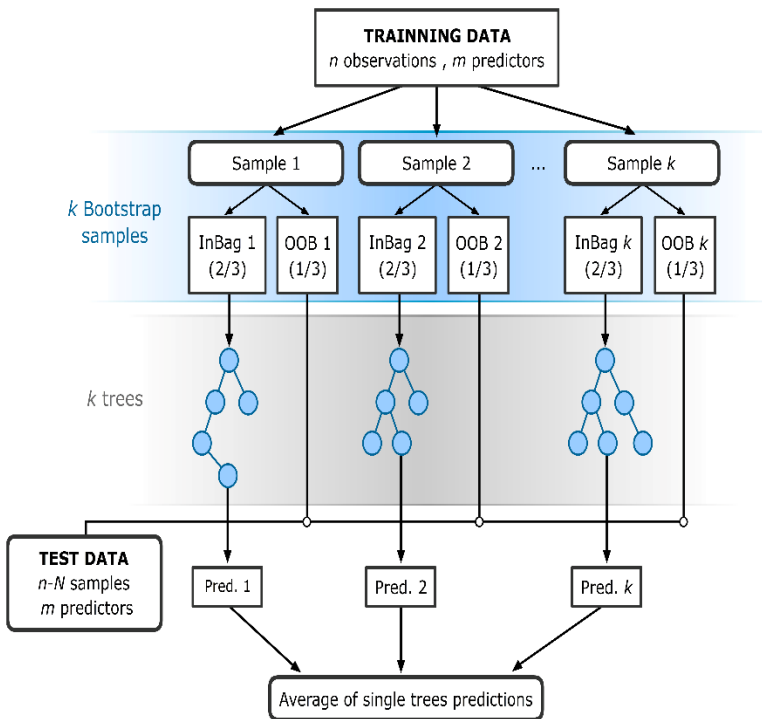


Figure 3. The flowchart of Random Forest for regression (adapted from Rodriguez-Galiano et al. 2015b). The RF method receives a subset of input vectors (n), made up of one phenology z-score value and the values of the corresponding weather predictors for a given location and year. RF builds a number K of regression trees making them grow from different training data subsets, resampling randomly the original dataset with replacement. Hence, most data will be used multiple times in different models. On the other hand, when the RF makes a tree grow, it uses the best predictor within a subset of predictors (m) which has been selected randomly from the overall set of input predictors. These especial characteristics of RF confer a greater prediction stability and accuracy and, at the same time, avoid the correlation of the different RTs, increasing the diversity of patterns that can be learnt from data. The multiple predictions of all k RTs for a given vector used as training are then averaged to obtain a unique estimation of the phenology z-score value.

### Section 3.5:

“...A feature selection approach, based on the ability of the RF to assess the relative importance of the predictors, was used to identify the minimum number of drivers which can better explain spring or autumn interannual variation in phenology. To assess the importance of each weather predictor, the RF switches one of the input predictors while keeping the rest constant, and it re-evaluates the performance of the model measuring the decrease in node impurity (Breiman, 2001). The differences were averaged over all 2000 trees to compute the general drivers for the interannual variation in Europe. However, different subsets of variables could be used to characterize different climates and ecological factors at every single regression tree model or node (see previous section). To reduce the number of drivers the least important predictor was removed iteratively at different steps. Then, a 5-fold cross-validation was applied to obtain a stable estimate of the error of the model built after predictor deletions. Finally, the model with a better trade-off between the number of predictors and error was chosen as the basis for interpreting the likely drivers of interannual variation in phenology.”

Comment 2: “Now, after you have mapped some model residuals, you should also use the information to critically discuss your work in the main text. If I interpret your supplementary graphs correctly they show distinct patterns, which shows that there is still systematic bias which needs to be carefully analysed, explained and discussed. This discussion should also include that the observed distribution of residuals might be an expression of heteroscedasticity which compromises the estimation of unbiased regression parameters.”

Reply 2: We would like to highlight that the validation of machine learning methods relies on the ability of the method to predict from new observations (independent test) that have not been used in the model building. Using the same training data would likely lead to an overestimation of the performance of the method. The way we have validated the models is therefore an unbiased estimation of the generalisation error. Additionally, we would like to highlight again that machine learning algorithms are non-linear, which implies that there are no assumptions/expectations about the distribution of the residuals (e.g. homoscedasticity).

It is true that the relative errors (from an independent test) for the multi-linear regression model seems to be heteroscedastic. However, this is supporting the initial hypotheses described in the manuscript: linear models might not be able to deal with the complex patterns between LSP and climate patterns at multiple locations and times, integrating them into a unique overall model.

The following paragraph has, thus, been included in the discussion section:

“The spatial distribution of the relative errors for RF and multivariate linear regression is shown in Figures S3 to S6 of the supporting information. The relative errors of the latter were significantly higher. Additionally, the residuals seemed not to be homoscedastic suggesting that linear models might not be able to deal with the complex

patterns between LSP and climate patterns at multiple locations and times, integrating them into a unique overall model.”

Comment 3: “The figure captions in the supplementary material are by far nor complete enough for understanding the figures (units, data sources, which test? ...). If you don’t exactly explain what you present, the presentation is useless. Please make sure that if it should come to a third revision to present it in appropriate quality.”

Reply 3: The figure captions in the supplementary material have been extended.

Comment 4: “I was surprised that the residuals maps are only limited to a small number of points, I guess, where you have ground observations. You trained the model with the satellite derived LSPs, so why don’t you present the residual maps that cover the entire continent.”

Reply 4: We have not used ground observations in this study. The Pan European Phenological Network (PEP725) mainly covers Germany and Austria, and the interannual variation in LSP occurs in many other different places. However, our LSP estimates (normal dates) were compared to those of PEP725 in a different study. Please see the following paragraph in Section 3.2:

“...These satellite-derived LSP estimates were compared to ground observations of the thousands of deciduous tree phenology records of the Pan European Phenology network (PEP725) (Rodriguez-Galiano et al., 2015a). This comparison resulted in a large spatio-temporal correlation of the phenology estimates with the spring phenophase (OG vs leaf unfolding; pseudo-R<sup>2</sup>=0.70) and autumn phenophase (EOS vs autumnal colouring; pseudo-R<sup>2</sup>=0.71).”

Regarding the origin of the residual maps, please see “reply 2” and the following paragraph in section 3.4 (Modelling interannual variation in LSP):

“The values of these variables at the selected years and locations (spatiotemporal model) were combined into a set of input feature vectors (3900 feature vectors for the spring model and 3124 for autumn) as an input to the RF algorithm. These feature vectors were divided equally into two subsets, one for the training of the models (inbag) and one as an additional test to the one internally computed by RF (out of bag; oob) to evaluate performance.”

Comment 5. Supporting strongly the point of Reviewer 2 on model selection (ref Figure 3): a) The selection of additional models should be depending on the gain of model performance (not necessarily on R<sup>2</sup> only). If the performance does not increase with increasing degrees of freedoms, using more complex models doesn’t make sense. b) Do you have any indication for the distribution of residuals or the RMSE having improved using more complex models.

Reply 5. We have not considered the determination coefficients only. Relative errors were decisive in the selection of the model. Please see the following paragraph (section 3.5) and Figure 3 of the current submission:

“In order to reduce the number of drivers the least important predictor was removed iteratively at different steps. Then, a 5-fold cross-validation was applied to obtain a stable estimate of the error of the model built after predictor deletions. Finally, the model with a better trade-off between number of predictors and error was chosen as the basis for interpreting the likely drivers of interannual variation in phenology.”

Comment 6. In Figures 5 the regressions are performed including two separated data domains (positive, negative fluctuations) . a) Why did you not use the entire data set including small and zero fluctuations? b) Please give the regressions for the variation within the domains. You will see the difference and will look at your results in a different way.

Reply 6. We would like to clarify that what we are showing in this figure is a scatterplot between the predicted values for an independent test (data that were not used in the regression model building; see previous comments) and the real values. This information is given as a complementary evaluation of the performance of the models, but it is not a regression model itself. This plot shows how our predictions deviate from the actual values in an independent dataset.

Regarding the inclusion of the zero values (no fluctuations) in the graph. It would not be possible, as the models have been trained for variation or changes and not for the “normal behaviour”. There are strong arguments against the inclusion of 0 values in the machine learning modelling process. Machine learning regression algorithms are “intelligent” and able to adapt to the data that are being modelled to minimize the generalisation error. On the other hand, no change occurrences are by far more abundant than changes. Consequently, the algorithms would focus on learning the patterns that explain no changes, rather than in patterns of changes. In other words, if we included zero values, an explanatory model of no-change would be obtained, which misses the point.

Comment 7. When you speak of ‘temporal variability’, it is interannual variability that you mean?

Reply 7. Yes, we have replaced “temporal variability” by “interannual variability”.

Comment 8. You speak several times of ‘biological scales’, without defining or explaining what you mean. In fact I don’t exactly understand what you want to say with this.

Reply 8. The concept “biological scales” has been defined in the text as follows:

“...On the other hand, many studies investigating the sensitivity of phenological events to climate variation use calendar seasonal or monthly mean climatic variables, which operate on fixed human calendar scales with a start date of 1<sup>st</sup> of January (Maignan et

al., 2008b), instead of using biological scales, for example, time relative to the growing phase of plants (Pau et al., 2011)."

1 **Modelling ~~temporal variation~~interannual variation in the**  
2 **spring and autumn land surface phenology of the**  
3 **European forest**

4

5 **V.F. Rodriguez-Galiano<sup>1,2</sup>, M. Sanchez-Castillo<sup>3</sup>, J. Dash<sup>2</sup>, P.M. Atkinson<sup>4,5,6,2</sup> and**  
6 **J. Ojeda-Zujar<sup>1</sup>**

7 [1] Physical Geography and Regional Geographic Analysis, University of Seville, Seville  
8 41004, Spain

9 [2] Global Environmental Change and Earth Observation Research Group, Geography and  
10 Environment, University of Southampton, Southampton SO17 1BJ, United Kingdom

11 [3] Department of Haematology, Wellcome Trust and MRC Cambridge Stem Cell Institute and  
12 Cambridge Institute for Medical Research, University of Cambridge, Cambridge CB2 0XY,  
13 United Kingdom

14 [4] Faculty of Science and Technology, Engineering Building, Lancaster University, Lancaster  
15 LA1 4YR, United Kingdom

16 [5] Faculty of Geosciences, University of Utrecht, Heidelberglaan 2, 3584 CS Utrecht, The  
17 Netherlands

18 [6] School of Geography, Archaeology and Palaeoecology, Queen's University Belfast, Belfast  
19 BT7 1NN, Northern Ireland, UK

20 Correspondence to: V.F. Rodriguez-Galiano (vrgaliano@us.esgmail.com)

21

22 **1. Abstract**

23 This research reveals new insights into the weather drivers of ~~temporal variation~~interannual  
24 variation in land surface phenology (LSP) across the entire European forest, while at the same

25 time establishes a new conceptual framework for predictive modelling of LSP. Specifically,  
26 the Random Forest method, a multivariate, spatially non-stationary and non-linear machine  
27 learning approach, was introduced for phenological modelling across very large areas and  
28 across multiple years simultaneously: the typical case for satellite-observed LSP. The RF  
29 model was fitted to the relation between LSP ~~temporal variation~~interannual variation and  
30 numerous climate predictor variables computed at biologically-relevant rather than human-  
31 imposed temporal scales. In addition, the legacy effect of an advanced or delayed spring on  
32 autumn phenology was explored. The RF models explained 81% and 62% of the variance in  
33 the spring and autumn LSP ~~temporal variation~~interannual variation, with relative errors of 10%  
34 and 20%, respectively: a level of precision that has until now been unobtainable at the  
35 continental scale. Multivariate linear regression models explained only 36% and 25%,  
36 respectively. It also allowed identification of the main drivers of the ~~temporal~~  
37 ~~variation~~interannual variation in LSP through its estimation of variable importance. This  
38 research, thus, shows an alternative to the hitherto applied linear regression approaches for  
39 modelling LSP and paves the way for further scientific investigation based on machine learning  
40 methods.

## 41 **2. Introduction**

42 Vegetation phenology has emerged as an important focus for scientific research in the last few  
43 decades. The interest in vegetation phenology is twofold: inter-annual recording of the timing  
44 of phenological events allows quantification of the impacts of climate change on vegetation;  
45 and a greater understanding of phenological responses enables meaningful projections of how  
46 ecosystems will respond to future changes in climate (Menzel, 2002; Morisette et al., 2008;  
47 Peñuelas, 2009; Peñuelas and Filella, 2001). Although different approaches have been devised  
48 for the study of vegetation phenology (Rafferty et al., 2013), the characterisation and modelling  
49 of vegetation phenology at global or regional scales has been undertaken mainly through the  
50 use of long-term time-series of satellite-sensor vegetation indices (termed land surface  
51 phenology, LSP, to reflect that satellite-observed phenology includes all land covers). Most  
52 studies of LSP analyse trends in phenological events across years (Delbart et al., 2008;  
53 Jeganathan et al., 2014; Jeong et al., 2011; Karlsen et al., 2007; Myneni et al., 1997), but more  
54 recent studies present process-based models to uncover cause-effect relationships between  
55 long-term trends in phenology and its key driving variables (Ivits et al., 012; Maignan et al.,  
56 2008a; Maignan et al., 2008b; Stöckli et al., 2011; Stöckli et al., 2008; Yu et al., 2015; Zhou et

57 al., 2001). This last group of studies focuses on trends in phenology produced by trends in  
58 weather (mainly warming). However, ~~temporal variation~~interannual variation in LSP arising  
59 as a consequence of the inter-annual variability in weather are less studied (Cook et al., 2005;  
60 De Beurs and Henebry, 2008; Menzel et al., 2005; Post and Stenseth, 1999; Zhang et al., 2004),  
61 with model-based studies of this phenomenon being scarce (van Vliet, 2010).

62 A higher frequency in the occurrence of extreme weather events has been observed in Europe,  
63 especially for summer temperatures (Barriopedro et al., 2011; Luterbacher et al., 2004). The  
64 summers of 2003 and 2010 in western and eastern Europe, respectively, were the warmest in  
65 the last 500 years (Barriopedro et al., 2011). Species and ecosystems respond more rapidly to  
66 these anomalies in weather than average climatic changes in most climatic scenarios (Zhao et  
67 al., 2013). Maignan et al. (2008b) and Rutishauser et al. (2008) reported that the LSP greening  
68 occurred 10 days earlier in 2007 than the average over the past three decades as a consequence  
69 of an exceptionally mild winter and spring. The study of the impacts of extreme inter-annual  
70 weather events on vegetation through the modelling of ~~temporal variation~~interannual variation  
71 in spring and autumn phenologies can increase our knowledge about climate-driven changes  
72 in phenology, acting as natural experiments in climate change scenarios (Rafferty et al., 2013).  
73 On the other hand, the modelling of LSP has been less explored compared to the modelling of  
74 individual plant species, and there are many aspects that remain to be understood, which limits  
75 comprehensive understanding of LSP and, therefore, of phenology at regional or global scales.  
76 A more complete modelling of LSP considering the inter-annual variation across large areas  
77 would include the capacity to interpret observations and make meaningful projections in  
78 relation to disturbances and their subsequent impacts (Morisette et al., 2008).

79 Modelling efforts to characterize LSP have generally relied on functions (usually linear) of  
80 meteorological drivers, such as average temperature and precipitation (Ivits et al., 2012),  
81 growing degree days (GDD) (de Beurs and Henebry, 2005), light and temperature (Stöckli et  
82 al., 2011), minimum temperature, photoperiod, vapour pressure deficit (Jolly et al., 2005;  
83 Stöckli et al., 2008), or minimum relative humidity (Brown and de Beurs, 2008). However,  
84 there is lack of understanding on number of important aspects, such as the multivariate  
85 influence of meteorological variables (temperature, precipitation, solar radiation) driving  
86 phenology, or the effect of additional drivers in the modelling of autumnal phenophases  
87 (Morisette et al., 2008). For instance, Fu et al. (2014) found a “cause-effect relationship”  
88 between an earlier leaf senescence and an earlier spring flushing in leaves of warmed samples  
89 of *Fagus sylvatica* and *Quercus robur*. This legacy effect of spring phenology has been

90 reported in recent studies using modified environments and plant species, but it has not been  
91 studied using LSP data. This latter aspect is particularly pertinent for studies that focus on inter-  
92 annual variation in phenology and could potentially contribute to increased knowledge of how  
93 climate change is affecting autumn phenology. On the other hand, many studies investigating  
94 the sensitivity of phenological events to climate variation use calendar seasonal or monthly  
95 mean climatic variables, which operate on fixed human calendar scales with a start date of 1<sup>st</sup>  
96 of January (Maignan et al., 2008b), instead of using biological scales, for example, time relative  
97 to the growing phase of plants~~daily data to build weather variables meaningful at biological~~  
98 ~~scales~~ (Pau et al., 2011). However, the modelling of interannual variation in LSP considering  
99 its potentially complicated relationship with climate in a multidimensional feature space (i.e.  
100 high number of multivariate weather drivers) might not be possible using traditional linear  
101 regression models (de Beurs and Henebry, 2005). In this sense, phenological modelling may  
102 benefit from machine learning techniques such as the Random Forest (RF) method (Breiman,  
103 2001), reducing uncertainties and bias (Zhao et al., 2013). RFs have the potential to identify  
104 and model the complex non-linear relationships between phenology and climate, being able to  
105 handle a large number of predictors and determine their importance in explaining phenology.  
106 RFs has been applied with very promising results to other fields of ecology and biological  
107 sciences (Archibald et al., 2009; Darling et al., 2012; Lawler et al., 2006), as well as to the  
108 simulation of phenological shifts under different climatic change scenarios (Lebourgeois et al.,  
109 2010), but the potential for modelling climate-driven ~~temporal variation~~interannual variation  
110 in phenology is still to be explored.

111 Understanding the effect of inter-annual weather variation on LSP is an essential step to  
112 establish a plausible link between recent climate variability and vegetation phenological  
113 responses at global or regional scales, and importantly to make reliable forecasts about future  
114 vegetation responses to different future climatic scenarios. The aim of this study is, therefore,  
115 to provide an explanation of the observed ~~temporal variation~~interannual variation in LSP of the  
116 entire European forest during the last decade, identifying the main weather drivers for spring  
117 and autumn at the continental scale. Our research offers new insights into the study of LSP by  
118 modelling the climate-driven past ~~temporal variation~~interannual variation in phenology, rather  
119 than trends, and using innovative multivariate non-linear machine learning techniques to  
120 evaluate multiple weather predictors at biological scales, and non-weather predictors such as  
121 the legacy effect of the date of spring onset in leaf senescence. Climate predictors used range  
122 from 30 days average values of temperature variables (max, min and avg) such as precipitation,

123 short wave radiation and day length; trimestral cumulated values such as growing degree days  
124 or chilling requirements, among others; to the date of specific events such as the first freeze or  
125 the last freeze. Moreover, we considered flexible biological time scales in the analysis between  
126 weather and phenological events rather than calendar months.

127

### 128 **3. Materials and Methods**

#### 129 **3.1 Data**

130 Three sources of data were used for this research: i) Satellite sensor derived temporal  
131 composites of MERIS Terrestrial Chlorophyll Index (MTCI), ii) temperature and precipitation  
132 data from the European Climate Assessment and Data (ECA&D) project (<http://www.ecad.eu>)  
133 and iii) surface radiation daylight (DAL;  $\text{w/m}^2$ ) data and surface incoming shortwave (SIS;  
134  $\text{w/m}^2$ ) radiation data from the Climate Monitoring Satellite Application Facilities (CM SAF,  
135 <http://www.cmsaf.eu>).

136 We used weekly composites of MTCI data at 1 km spatial resolution from 2002 to 2012. This  
137 dataset was supplied by the European Space Agency and processed by Airbus Defence and  
138 Space. Daily temperature (mean, minimum and maximum) and daily precipitation data were  
139 derived from the European Climate Assessment & Dataset (ECA&D) time-series (version 10.0)  
140 with spatial resolution of  $0.25^\circ \times 0.25^\circ$ , covering the period from 2002 to 2011 (Haylock et al.,  
141 2008). The CM SAF DAL version CDR v001 (Müller and Trentmann, 2013) and SIS version  
142 CDR v002 (Posselt et al., 2012; Posselt et al., 2011) were derived from Meteosat satellite  
143 sensors at a spatial resolution of  $0.05^\circ \times 0.05^\circ$  covering the same period as ECA&D.

#### 144 **3.2 Phenology extraction and ~~temporal variation~~interannual variation in LSP** 145 **computation**

146 The time-series of MERIS MTCI data was used to estimate both the onset of greenness  
147 (OG) and end of senescence (EOS) from 2003 to 2011. Data for every estimation year  
148 considered 1.5 years of data (from October in the previous year to July in the next year)  
149 because the annual pattern of vegetation growth in some parts of Europe spans across  
150 calendar years and, hence, insufficient information about LSP is captured using a single  
151 year of data. The yearly values of OG and EOS were estimated for each image pixel of the

152 study area using the methodology described in Dash et al. (2010). This methodology  
153 consists of two major procedures: data smoothing and LSP estimation (Figure 2a).  
154 Smoothed MTCI time-series data were obtained using a discrete Fourier transform because  
155 of its advantage of requiring fewer user-defined parameters compared to other methods  
156 (Atkinson et al., 2012). The peak in the annual profile was defined as a point on the  
157 phenological curve where the first derivative changes sign from positive to negative. Next,  
158 the derived data were searched backward and forward departing from the maximum annual  
159 peak to estimate the OG and EOS, respectively. OG was defined as a valley at the  
160 beginning of the growing season point (a change in derivative value from positive to  
161 negative) and EOS was defined as a valley point occurring at the decaying end of a  
162 phenology cycle (a change in derivative value from negative to positive). These satellite-  
163 derived LSP estimates were compared to ground observations of the thousands of  
164 deciduous tree phenology records of the Pan European Phenology network (PEP725)  
165 (Rodriguez-Galiano et al., 2015a). This comparison resulted in a large spatio-temporal  
166 correlation of the phenology estimates with the spring phenophase (OG vs leaf unfolding;  
167 pseudo- $R^2=0.70$ ) and autumn phenophase (EOS vs autumnal colouring; pseudo- $R^2=0.71$ ).

168 Z-score values during the study period were used as a proxy to measure ~~temporal~~  
169 ~~variation~~interannual variation in the LSP parameters. The z-score values for a given year  
170 were defined as the difference from the multi-year mean, normalized by the standard  
171 deviation across years. The value of the targeted year was excluded in the computation of  
172 multiyear mean to enhance the inter-annual variation (Saleska et al., 2007). The spatio-  
173 temporal distribution of spring and autumn LSP z-score values is shown in Figures S1 and  
174 S2 of the supporting information, respectively.

175 To match the spatial resolution of the ECA&D dataset, the LSP z-score values for each year  
176 were resampled to a spatial resolution of  $0.25^\circ \times 0.25^\circ$  by calculating the median of all the LSP  
177 z-score values within this area after excluding the areas with fewer than 50 LSP estimates and  
178 the non-forest pixels according to the Globcover2005 and Globcover2009 land cover maps  
179 (<http://due.esrin.esa.int/globcover/>). Only LSP estimates with complete temporal coverage  
180 (2003–2011) were included in the analysis to reduce the likelihood of natural and human  
181 disturbances (Potter et al., 2003). Globcover was selected for its greater consistency with the  
182 MERIS MTCI time-series and its high geolocational accuracy (<150 m) (Bicheron et al., 2011).

183 **3.3 Computation of weather predictors**

184 A suite of weather predictors were computed for each  $0.25 \times 0.25^\circ$  grid cell associated with the  
185 occurrence of positive or negative z-score values in LSP based on the ECA&D and CM SAF  
186 datasets (see Table 1). The predictors include temporal average values of temperature variables  
187 (Tmax, Tmin and Tavg), precipitation, DAL and SIS; temporal cumulated predictors such as  
188 growing degree days, chilling, precipitation, SIS and DAL; and the date of specific events such  
189 as the onset of greenness (legacy effect for autumn phenology modelling) the first freeze or the  
190 last freeze, as well as the difference between both dates (freeze period) for the modelling of  
191 autumn only. Growing degree days were computed using temperature thresholds of  $0^\circ$  and  $5^\circ$ .  
192 Chilling requirements were computed as the sum of negative temperatures (temperatures below  
193  $0^\circ$ ). Freeze was defined as dates with minimum temperatures lower than  $-2^\circ$  (Schwartz et al.,  
194 2006).

195 The different weather predictors were computed based on the 30 and 90 days previous to the  
196 day of the year (DOY) of the z-score values in OG and EOS (Figure 2b) following Schwartz  
197 et al. (2006) and Menzel et al. (2006), who found that most phenophases of plant observations  
198 in Europe correlated significantly with weather predictors representing the month of onset and  
199 the two preceding months. The chilling requirements for spring modelling and freeze predictors  
200 were an exception, as the period for its computation starts 90 days prior to the OG. Relative  
201 differences between each predictor and its multi-year average for the same period were  
202 computed to capture the inter-annual variability in climate variables at the pixel level for every  
203 predictor and to facilitate the modelling of climate-driven variation in phenology (Table 1).

204 **3.4 Modelling temporal variationinterannual variation in LSP**

205 ~~Conventional statistical models such as linear regression might be inappropriate for  
206 investigating the drivers of interannual variation in phenology because many of the  
207 relationships are likely to be non-linear (De Beurs and Henebry, 2008). In this sense, machine  
208 learning methods have emerged as complementary alternatives to conventional statistical  
209 techniques. Within the branch of machine learning techniques, regression trees are particularly  
210 suitable when compared to global single predictive models, allowing for multiple regression  
211 models using recursive partitioning (Breiman, 1984). Assembling a single global model might  
212 not be representative of LSP of the entire European continent, when there are many climatic  
213 drivers which interact in complicated, non-linear ways and may vary spatially and temporally.~~

214 For the purpose of this paper, an alternative approach is to sub-divide, or partition, the data  
215 space into more homogeneous regions of similar climates and ecological factors.

216 Regression trees use a sum of squares criterion to split the data into successively more  
217 homogeneous subsets contained at many different structural units called nodes. Each of the  
218 terminal nodes, has attached to it a simple regression which applies in that node only. Therefore,  
219 different regressions can be fitted to different data subsets within one single regression tree,  
220 which can represent different responses controlled by different drivers (Archibald et al., 2009;  
221 Lawler et al., 2006). Additionally, the performance of multiple regression trees can be  
222 combined to increase the predictive ability of a single regression tree model, following the  
223 Random Forest technique (Figure 3). The RF method is an innovative machine learning  
224 approach that can perform multivariate non-linear regression, combining the performance of  
225 numerous regression tree algorithms to predict the interannual variation in OG and EOS. More  
226 details regarding the performance and the specific characteristics of a RF model can be seen in  
227 Rodriguez-Galiano et al. (2015b); Rodriguez-Galiano et al. (2014), and Figure 3.

228 The Random Forest method was applied to phenological modelling across very large areas and  
229 across multiple years simultaneously: the typical case for satellite-observed LSP. The RF  
230 model was fitted to the relation between LSP interannual variation and numerous climate  
231 predictor variables computed at biologically-relevant rather than human-imposed temporal  
232 scales. We restricted our climate data choices to daily data (average, minimum and maximum  
233 temperatures, precipitation and radiation) to account for integrative forcing (that is, growing  
234 degree days, chilling requirements as well as cumulative precipitation and radiation), computed  
235 from the exact day of the phenological event backwards, rather than using the calendar months.  
236 The locations with z-score in LSP greater than 1 (positive and negative) were selected to build  
237 a RF predictive model on OG and EOS. Z-score values of OG or EOS for each year were  
238 combined together with the different weather predictors. The z-score values in OG were  
239 assessed as an extra predictor to evaluate the legacy effect of an advanced or delayed spring in  
240 the modelling of EOS. The values of these variables at the selected years and locations  
241 (spatiotemporal model) were combined into a set of input feature vectors (3900 feature vectors  
242 for the spring model and 3124 for autumn) as an input to the RF algorithm. These feature  
243 vectors were divided equally into two subsets, one for the training of the models (inbag) and  
244 one as an additional test to the one internally computed by RF (out of bag; oob) to evaluate  
245 performance. RF models composed of 2000 trees were grown using different subsets of  
246 predictors, varying the number of random predictors from 1 to 9. The Random Forest method

247 within the package implemented in the R statistical software was used to build the different  
248 models (Liaw and Wiener, 2002). ~~onventional statistical models such as linear regression might~~  
249 ~~be inappropriate for investigating the drivers of temporal variation in phenology because many~~  
250 ~~of the relationships are likely to be non linear (De Beurs and Henebry, 2008).~~ In this sense,  
251 ~~machine learning methods have emerged as complementary alternatives to conventional~~  
252 ~~statistical techniques. Within the branch of machine learning techniques, regression trees are~~  
253 ~~particularly suitable when compared to global single predictive models, allowing for multiple~~  
254 ~~regression models using recursive partitioning (Breiman et al., 1984).~~ Assembling a single  
255 ~~global model might not be representative of the phenomenon under study when there are many~~  
256 ~~predictors which interact in complicated, non linear ways and may vary spatially and~~  
257 ~~temporally. An alternative approach is to sub-divide, or partition, the space into more~~  
258 ~~homogeneous regions of similar characteristics. Regression trees use a sum of squares criterion~~  
259 ~~to split the data into successively more homogeneous subsets. Therefore, different regression~~  
260 ~~models can be fitted to different data subsets, which can represent different responses~~  
261 ~~controlled by different drivers (Archibald et al., 2009; Lawler et al., 2006).~~ For the purpose of  
262 ~~this paper, this latter property makes regression trees particularly advantageous.~~

263 Different approaches have been proposed in the last few years to increase the predictive ability  
264 ~~of regression tree models. Among all of them RFs are probably the most popular technique due~~  
265 ~~to the simplicity of their applicability, interpretability of the models, and the robustness of~~  
266 ~~predictions (Rodriguez-Galiano et al., 2015b).~~ The RF method is an innovative machine  
267 ~~learning approach that can perform multivariate non linear regression, combining the~~  
268 ~~performance of numerous regression tree algorithms to predict the temporal variation in OG~~  
269 ~~and EOS. The RF method receives a subset of  $(x)$  input vectors, made up of one phenology z-~~  
270 ~~score value and the values of the corresponding weather predictors considered in the regression.~~  
271 ~~RF builds a number  $K$  of regression trees (individual regression models) and averages the~~  
272 ~~results (Breiman, 2001).~~ After  $K$  such trees  $\{T(x)\}_1^K$  are grown, the RF regression predictor  
273 ~~becomes:~~

$$\hat{f}_{rf}^K(x) = \frac{1}{K} \sum_{k=1}^K T(x)$$

274  
275 ~~More details regarding the performance and the specific characteristics of a RF model can be~~  
276 ~~seen in Rodriguez-Galiano et al. (2015b); Rodriguez-Galiano et al. (2014).~~

277 Random Forest method was applied to phenological modelling across very large areas and  
278 across multiple years simultaneously: the typical case for satellite-observed LSP. The RF  
279 model was fitted to the relation between LSP temporal variation and numerous climate  
280 predictor variables computed at biologically relevant rather than human imposed temporal  
281 scales. We restricted our climate data choices to daily data (average, minimum and maximum  
282 temperatures, precipitation and radiation) to account for integrative forcing (that is, growing  
283 degree days, chilling requirements as well as cumulative precipitation and radiation), computed  
284 from the exact day of the phenological event backwards, rather than using the calendar months  
285 of the calendar months. The locations with z-score in LSP greater than 1 (positive and negative)  
286 were selected to build a RF predictive model on OG and EOS. Z-score values of OG or EOS  
287 for each year were combined together with the different weather predictors. The z-score values  
288 in OG were assessed as an extra predictor to evaluate the legacy effect of an advanced or  
289 delayed spring in the modelling of EOS. The values of these variables at the selected years and  
290 locations (spatiotemporal model) were combined into a set of input feature vectors (3900  
291 feature vectors for the spring model and 3124 for autumn) as an input to the RF algorithm.  
292 These feature vectors were divided equally into two subsets, one for the training of the models  
293 and one as an additional test to the one internally computed by RF (out of bag; oob) to evaluate  
294 performance. RF models composed of 2000 trees were grown using different subsets of  
295 predictors, varying the number of random predictors from 1 to 9. Random Forest method within  
296 the package implemented in the R statistical software was used to build the different models  
297 (Liaw and Wiener, 2002).

### 298 3.5 Selection of the most important predictors

299 The RF method can use the oob subset to estimate the relative importance of each predictor in  
300 the model. This property is especially useful for the present research, but also for other  
301 multivariate biological studies, where it is important to know the physical drivers of the  
302 phenomenon under investigation (Archibald et al., 2009; Lawler et al., 2006). However, the  
303 inclusion of different measures of weather predictors may imply a large increase in the  
304 dimensionality of the datasets being used, as these variables are obtained by applying multiple  
305 functions or measures to the temperature, precipitation and radiation time-series. On the one  
306 hand, more information may be useful for the modelling process; on the other hand, an  
307 excessive number of correlated predictors or features can overwhelm the expected increase in  
308 accuracy and may introduce additional complexity limiting the ability of the method to point

309 to possible cause-effect relationships between ~~temporal variation~~interannual variation in  
310 phenology and their drivers, making interpretation challenging.

311 ~~A feature selection approach, based on the ability of the RF to assess the relative importance~~  
312 ~~of the predictors, was used to identify the minimum number of drivers which can better explain~~  
313 ~~spring or autumn interannual variation in phenology. To assess the importance of each weather~~  
314 ~~predictor, the RF switches one of the input predictors while keeping the rest constant, and it re-~~  
315 ~~evaluates the performance of the model measuring the decrease in node impurity~~ (Breiman,  
316 2001).~~The differences were averaged over all 2000 trees to compute the general drivers for the~~  
317 ~~interannual variation in Europe. However, different subsets of variables could be used to~~  
318 ~~characterize different climates and ecological factors at every single regression tree model or~~  
319 ~~node (see previous section). In order to reduce the number of drivers the least important~~  
320 ~~predictor was removed iteratively at different steps. Then, a 5-fold cross-validation was applied~~  
321 ~~to obtain a stable estimate of the error of the model built after predictor deletions. Finally, the~~  
322 ~~model with a better trade-off between number of predictors and error was chosen as the basis~~  
323 ~~for interpreting the likely drivers of interannual variation in phenology.~~~~A feature selection~~  
324 ~~approach, based on the ability of the RF to assess the relative importance of the predictors, was~~  
325 ~~used to identify the minimum number of drivers which can better explain spring or autumn~~  
326 ~~temporal variation in phenology. To assess the importance of each weather predictor, the RF~~  
327 ~~switches one of the input predictors while keeping the rest constant, and it re-evaluates the~~  
328 ~~performance of the model measuring the decrease in node impurity~~ (Breiman, 2001).~~The~~  
329 ~~differences were averaged over all 2000 trees. In order to reduce the number of drivers the least~~  
330 ~~important predictor was removed iteratively at different steps. Then, a 5-fold cross-validation~~  
331 ~~was applied to obtain a stable estimate of the error of the model built after predictor deletions.~~  
332 ~~Finally, the model with a better trade-off between number of predictors and error was chosen~~  
333 ~~as the basis for interpreting the likely drivers of temporal variation in phenology.~~

334 **4. Results**

335 Numerous models were built on the basis of different predictor combinations considering  
336 different temporal windows prior to the spring and autumn phenological events (see section  
337 “computation of weather predictors”). The percentage of variation (pseudo- $R^2$ ) explained by  
338 different weather-LSP models is shown in the supplementary information (Table S1, S2 and  
339 S3). No previous studies have investigated in depth the parametrization of GDD for LSP and  
340 climate inter-comparison, unlike for ground phenological studies (Snyder et al., 1999).

341 Although, we did not carry out an exhaustive analysis of the optimum GDD parametrization,  
342 our results showed a systematic pattern in spring models, presenting slightly larger pseudo- $R^2$   
343 for models which used 0° C as a threshold for the computation of GDD (rather than 5° C).  
344 Regarding, the length of the temporal windows for weather function computation, spring  
345 models using 30 and 90 days for the computation of averaged and cumulative functions were  
346 more accurate, whereas for autumn models with 90 day-averaged predictors outperformed the  
347 rest.

348 The main drivers of ~~temporal variation~~interannual variation in LSP were identified through the  
349 application of a feature selection procedure (see section “selection of the most important  
350 predictors”). Spring models were more accurate than autumn, with median relative error values  
351 of 10% to 27% (12 to 1 predictor), versus 26% to 60% of autumn (14 to 1 predictor). Figure  
352 43 shows the pseudo- $R^2$  of the models as well as the relative importance of each predictor.  
353 Spring models explained a percentage of the variance up to 81% (Figure 43a), whereas autumn  
354 explained up to 61% (Figure 43b). Cook et al. (2005), using a modelled based on GDD only,  
355 explained 63% on the variance of onset date for mixed and boreal forest. Figure 54 shows the  
356 relative error in the prediction of different models after removing the least important predictor.  
357 Regarding the relative importance of the drivers, the same ranking in importance was observed  
358 within the different models of each phenophase, which reflected the stability in the RF  
359 importance estimation, and a high reliability of the results (Figure 43). To interpret the main  
360 weather drivers of the ~~temporal variation~~interannual variation in phenology, simplified models  
361 with reduced number of predictors were selected for spring and autumn (see section 3.5),  
362 respectively. The spring model was composed of 6 predictors (pseudo- $R^2$ =0.77 and median  
363 relative error of 10%) and the autumn model of 5 predictors (pseudo- $R^2$ =0.59 and median  
364 relative error of 28%) (Figure 65). Our results suggest that ~~temporal variation~~interannual  
365 variation in the onset on greenness (LSP) of temperate forest species are driven mainly by the  
366 daily temperature of the 30 days prior to onset (but not necessarily the GDD), with the most  
367 important driver being the minimum temperature. Photoperiod was also important, the most  
368 accurate empirical prediction was obtained by a combined temperature-radiation forcing,  
369 integrating the SIS of the previous 90 days. For senescence, temperature was suggested to be  
370 more important than photoperiod in controlling the senescence process (Archetti et al., 2013;  
371 Jeong and Medvigy, 2014; Vitasse et al., 2009; Yang et al., 2012), with the most important  
372 drivers being the date of the first freeze and the accumulation of chilling temperatures.  
373 However, we did not observe a legacy effect of a much earlier or later spring onset on the date

374 of senescence. Autumn models that included the ~~temporal variation~~interannual variation (z-  
375 score values) in the onset of greenness did not outperform the remaining models (see Table S2  
376 and S3 in supplementary information) and the relative importance was low in comparison with  
377 other drivers.

378 **5. Discussion**

379 The selection and computation of the weather predictors is an important step of phenological  
380 modelling. Most of studies on the sensitivity of phenological events to climate used human  
381 calendar scales, that is, seasonal or monthly calendar mean or cumulative climate predictors  
382 (Maignan et al., 2008a; Maignan et al., 2008b; Menzel et al., 2006; Schwartz et al., 2006),  
383 overlooking the importance of biological time-scales in phenology. However, with the  
384 increased availability of daily weather datasets, current and future studies might benefit from  
385 the use of daily information to model the drivers of plants' circadian time-scales (Pau et al.,  
386 2011). Our study advanced the modelling of vegetation phenology by improving the temporal  
387 matching between LSP ~~temporal variation~~interannual variation and the preceding weather  
388 conditions by analysing daily data at biological scales. Regarding, the length of the temporal  
389 windows for weather function computation, Menzel et al. (2006) showed that most  
390 phenological phases of plant species in Europe correlate significantly with mean temperatures  
391 of the month of onset and the two preceding months. However, in our study, when end of  
392 senescence was considered, a consistent divergent effect was observed between spring and  
393 autumn. Autumn phenophases might be driven by longer-term changes in weather, while for  
394 spring the average conditions of the 30 days previous to the date of onset play a more important  
395 role (Table S1, S2 and S3 in supplementary information). From a computational point of view,  
396 considering larger temporal windows for calculating averages would induce a smoothing effect,  
397 degrading the information in the predictors, whereas cumulative functions such as GDD or  
398 chilling requirements would not be affected by this effect. However, we observed a divergent  
399 response between spring and autumn and consistent throughout the models of each phenophase  
400 suggests that a biological explanation for this phenomenon might be plausible.

401 Understanding the drivers of ~~temporal variation~~interannual variation in LSP amidst  
402 background inter-annual variation is a critical aspect of global change science (de Beurs and  
403 Henebry, 2005; Zhao et al., 2013). To this end, the RF method is particularly pertinent, as it  
404 allows the assessment of the importance of the predictors (Figure 43). Our findings reveal that  
405 the accuracy of growing degree day-based models might be overestimated using linear

406 regression models and that non-linear multivariate relationships between temperature  
407 (especially minimum temperature) and radiation are needed to describe the relations between  
408 phenology and weather drivers. This supports the findings of Stöckli et al. (2011) who  
409 explained temperate phenology using a combination of light and temperature. The highlighted  
410 importance of minimum temperatures might be related to the fact that minimum temperature  
411 is a better indicator of weather changes than either the average or maximum temperature  
412 (Duncan et al., 2014; Jolly et al., 2005). Regarding GDD, although it has been applied  
413 extensively to predict vegetation phenophases, it is currently debated whether such models can  
414 detect when multiple environmental drivers are required to initiate a phenological event, or  
415 detect drivers that are relatively static across time, such as photoperiod (Stöckli et al. 2011).  
416 Our results reveal that multiple environmental drivers are required to initiate phenological  
417 events of Europe and also showed that the role of GDD alone in driving spring phenology  
418 might be overestimated due to an over-reliance on linear models. GDD had the largest linear  
419 association with vegetation phenology ~~temporal variation~~interannual variation, while the linear  
420 correlation between LSP and others drivers that were revealed as very important by the RF was  
421 small (see Tables 1 and 2). A simple linear analysis between GDD and phenology could ignore  
422 complex non-linear associations between phenology and predictors as well as synergies  
423 between weather drivers. Regarding the senescence phase, the autumn models had a weaker  
424 predictive power compared the spring models. There is still lack of clear understanding of  
425 mechanism autumn senescence, however, temperature, and particularly the dates of freeze, has  
426 been suggested as major driver for autumn phenology.

427 The RF method provided an important alternative over simple, but less accurate analysis based  
428 on linear regression for the analysis of ~~temporal variation~~interannual variation in spring and  
429 autumn phenology. A further comparison with a linear regression analysis suggested that there  
430 might be a non-linear relationship between the ~~temporal variation~~interannual variation in LSP  
431 and the weather drivers. Multivariate linear regression models were also fitted from the same  
432 combination of predictors selected as optimal by Random Forest. Multivariate linear models  
433 explained only 36% and 26% of the variance in spring and autumn phenology ~~temporal~~  
434 variationinterannual variation across the continental scale. Additionally, a linear regression  
435 between predicted values from RF and observed ~~temporal variation~~interannual variation in  
436 phenology produced  $R^2$  values equal to 0.90 and 0.68 for spring and autumn LSP ~~temporal~~  
437 variationinterannual variation, respectively (Figure 65a and 64b). On the other hand, the  
438 correlations between the predictions of linear regression models and observations were much

439 weaker, with  $R^2$  values of 0.39 and 0.25 (Figure 65c and 65d). Linear models under-predicted  
440 a delay in the phenophases (positive z-score values) and over-predicted the advances (negative  
441 z-score values). The spatial distribution of the relative errors for RF and multivariate linear  
442 regression is shown in Figures S3 to S6 of the supporting information. The relative errors of  
443 the latter were significantly higher. Additionally, the residuals seemed not to be homoscedastic  
444 suggesting that linear models might not be able to deal with the complex patterns between LSP  
445 and climate patterns at multiple locations and times, integrating them into a unique overall  
446 model.

447 A new approach to model ~~temporal variation~~interannual variation in LSP was presented in this  
448 paper based on the application of the RF model to a set of climate predictors at biological scales.  
449 This new modelling technique has numerous advantages for the modelling of climate-driven  
450 ~~temporal variation~~interannual variation in LSP. It is a non-parametric multivariate method  
451 which allows for non-linear relationships between (compared to traditional linear models)  
452 phenology and climate and can consider a large number of weather predictors in the modelling  
453 process. This provides potential opportunity to capture the impact of all possible  
454 environmental/weather drivers on vegetation phenology. The proposed method can recognize  
455 complex patterns between LSP and climate at multiple locations and times, integrating them  
456 into a unique overall model, rather than generating multiple models over a geographical area  
457 and for different years. Additionally it is data-driven, which means that there is no need to  
458 incorporate previous knowledge about the specific responses of vegetation to different  
459 predominant weather controls (i.e. temperature, rainfall, and photoperiod), allowing weather  
460 drivers to automatically shift both temporally and spatially. Therefore, it is highly generalizable,  
461 being applicable to different biogeographical regions where the phenology is controlled by  
462 different factors. This flexibility or generalization capacity of RF models to transition from one  
463 driver to another without the need for a model change also promotes its application to different  
464 climate change scenarios. We succeeded in modelling the ~~temporal variation~~interannual  
465 variation in LSP phenology as observed from satellite-sensors in the European Forest, while  
466 using the same type of input data, the same model, and the same model parameters for the  
467 entire European continent.

468 **Author Contributions**

469 V.F.R.G., J.D. and P.M.A. conceived and designed the experiments; V.F.R.G. performed the  
470 experiments; V.F.R.G., M.S.C. and J.D. contributed analysis tools; V.F.R.G. drafted the paper.  
471 All authors contributed to the final paper.

472 **Acknowledgements**

473 The first author is a Marie Curie Grant holder (reference FP7-PEOPLE-2012-IEF-331667).  
474 The authors are grateful for the financial support given by the European Commission under the  
475 Seventh Framework Programme and the Spanish MINECO (project BIA2013-43462-P). PMA  
476 is grateful to the University of Utrecht for supporting him with The Belle van Zuylen Chair.  
477 We acknowledge the E-OBS dataset from the EU-FP6 project ENSEMBLES  
478 (<http://ensembles-eu.metoffice.com>) and the data providers in the ECA&D project  
479 (<http://www.ecad.eu>)". Surface radiation data were obtained from EUMETSAT's Satellite  
480 Application Facility on Climate Monitoring (CM SAF).

481 **References**

482 Archetti, M., Richardson, A. D., O'Keefe, J., and Delpierre, N.: Predicting Climate Change Impacts on  
483 the Amount and Duration of Autumn Colors in a New England Forest, *PLoS ONE*, 8, 2013.  
484 Archibald, S., Roy, D. P., van Wilgen, B. W., and Scholes, R. J.: What limits fire? An examination of  
485 drivers of burnt area in Southern Africa, *Glob. Change Biol.*, 15, 613-630, 2009.  
486 Atkinson, P. M., Jeganathan, C., Dash, J., and Atzberger, C.: Inter-comparison of four models for  
487 smoothing satellite sensor time-series data to estimate vegetation phenology, *Remote Sens. Environ.*,  
488 123, 400-417, 2012.  
489 Barriopedro, D., Fischer, E. M., Luterbacher, J., Trigo, R. M., and García-Herrera, R.: The Hot Summer  
490 of 2010: Redrawing the Temperature Record Map of Europe, *Science*, 332, 220-224, 2011.  
491 Bicheron, P., Amberg, V., Bourg, L., Petit, D., Huc, M., Miras, B., Brockmann, C., Hagolle, O., Delwart,  
492 S., Ranera, F., Leroy, M., and Arino, O.: Geolocation Assessment of MERIS GlobCover Orthorectified  
493 Products, *IEEE Trans. Geosci. Remote Sensing*, 49, 2972-2982, 2011.  
494 Breiman, L.: Classification and regression trees, Chapman & Hall/CRC, 1984.  
495 Breiman, L.: Random forests, *Machine Learning*, 45, 5-32, 2001.  
496 Brown, M. E. and de Beurs, K. M.: Evaluation of multi-sensor semi-arid crop season parameters based  
497 on NDVI and rainfall, *Remote Sens. Environ.*, 112, 2261-2271, 2008.  
498 Cook, B. I., Smith, T. M., and Mann, M. E.: The North Atlantic Oscillation and regional phenology  
499 prediction over Europe, *Glob. Change Biol.*, 11, 919-926, 2005.  
500 Darling, E. S., Alvarez-Filip, L., Oliver, T. A., McClanahan, T. R., and Côté, I. M.: Evaluating life-history  
501 strategies of reef corals from species traits, *Ecology Letters*, 15, 1378-1386, 2012.  
502 Dash, J., Jeganathan, C., and Atkinson, P. M.: The use of MERIS Terrestrial Chlorophyll Index to study  
503 spatio-temporal variation in vegetation phenology over India, *Remote Sens. Environ.*, 114, 1388-1402,  
504 2010.  
505 de Beurs, K. M. and Henebry, G. M.: Land surface phenology and temperature variation in the  
506 International Geosphere-Biosphere Program high-latitude transects, *Glob. Change Biol.*, 11, 779-790,  
507 2005.

508 De Beurs, K. M. and Henebry, G. M.: Northern annular mode effects on the land surface phenologies  
509 of northern Eurasia, *Journal of Climate*, 21, 4257-4279, 2008.

510 Delbart, N., Picard, G., Le Toan, T., Kergoat, L., Quegan, S., Woodward, I., Dye, D., and Fedotova, V.:  
511 Spring phenology in boreal Eurasia over a nearly century time scale, *Glob. Change Biol.*, 14, 603-614,  
512 2008.

513 Duncan, J. M. A., Dash, J., and Atkinson, P. M.: Elucidating the impact of temperature variability and  
514 extremes on cereal croplands through remote sensing, *Glob. Change Biol.*, 21, 1541-1551, 2014.

515 Fu, Y. S. H., Campioli, M., Vitassee, Y., De Boeck, H. J., Van Den Berge, J., AbdElgawad, H., Asard, H., Piao,  
516 S., Deckmyn, G., and Janssens, I. A.: Variation in leaf flushing date influences autumnal senescence  
517 and next year's flushing date in two temperate tree species, *Proceedings of the National Academy of  
518 Sciences of the United States of America*, 111, 7355-7360, 2014.

519 Haylock, M. R., Hofstra, N., Klein Tank, A. M. G., Klok, E. J., Jones, P. D., and New, M.: A European daily  
520 high-resolution gridded data set of surface temperature and precipitation for 1950-2006, *J. Geophys.  
521 Res.*, 113, 2008.

522 Ivits, E., Cherlet, M., Tóth, G., Sommer, S., Mehl, W., Vogt, J., and Micale, F.: Combining satellite  
523 derived phenology with climate data for climate change impact assessment, *Global and Planetary  
524 Change*, 88-89, 85-97, 012.

525 Ivits, E., Cherlet, M., Tóth, G., Sommer, S., Mehl, W., Vogt, J., and Micale, F.: Combining satellite  
526 derived phenology with climate data for climate change impact assessment, *Glob. Planet. Change*, 88-  
527 89, 85-97, 2012.

528 Jeganathan, C., Dash, J., and Atkinson, P. M.: Remotely sensed trends in the phenology of northern  
529 high latitude terrestrial vegetation, controlling for land cover change and vegetation type, *Remote  
530 Sens. Environ.*, 143, 154-170, 2014.

531 Jeong, S.-J., Ho, C.-H., Gim, H.-J., and Brown, M. E.: Phenology shifts at start vs. end of growing season  
532 in temperate vegetation over the Northern Hemisphere for the period 1982–2008, *Glob. Change Biol.*,  
533 17, 2385-2399, 2011.

534 Jeong, S.-J. and Medvigy, D.: Macroscale prediction of autumn leaf coloration throughout the  
535 continental United States, *Global Ecology and Biogeography*, 23, 1245-1254, 2014.

536 Jolly, W. M., Nemani, R., and Running, S. W.: A generalized, bioclimatic index to predict foliar  
537 phenology in response to climate, *Glob. Change Biol.*, 11, 619-632, 2005.

538 Karlsen, S. R., Solheim, I., Beck, P. S. A., Hogda, K. A., Wielgolaski, F. E., and Tommervik, H.: Variability  
539 of the start of the growing season in Fennoscandia, 1982-2002, *Int. J. Biometeorol.*, 51, 513-524, 2007.

540 Lawler, J. J., White, D., Neilson, R. P., and Blaustein, A. R.: Predicting climate-induced range shifts:  
541 Model differences and model reliability, *Glob. Change Biol.*, 12, 1568-1584, 2006.

542 Lebourgais, F., Pierrat, J. C., Perez, V., Piedallu, C., Cecchini, S., and Ulrich, E.: Simulating phenological  
543 shifts in French temperate forests under two climatic change scenarios and four driving global  
544 circulation models, *Int. J. Biometeorol.*, 54, 563-581, 2010.

545 Liaw, A. and Wiener, M.: Classification and Regression by randomForest, *R News*, 2/3, 18-22, 2002.

546 Luterbacher, J., Dietrich, D., Xoplaki, E., Grosjean, M., and Wanner, H.: European Seasonal and Annual  
547 Temperature Variability, Trends, and Extremes Since 1500, *Science*, 303, 1499-1503, 2004.

548 Maignan, F., Bréon, F. M., Bacour, C., Demarty, J., and Poirson, A.: Interannual vegetation phenology  
549 estimates from global AVHRR measurements: Comparison with in situ data and applications, *Remote  
550 Sens. Environ.*, 112, 496-505, 2008a.

551 Maignan, F., Bréon, F. M., Vermote, E., Ciais, P., and Viovy, N.: Mild winter and spring 2007 over  
552 western Europe led to a widespread early vegetation onset, *Geophys. Res. Lett.*, 35, L02404, 2008b.

553 Menzel, A.: Phenology: Its Importance to the Global Change Community, *Clim. Change*, 54, 379-385,  
554 2002.

555 Menzel, A., Sparks, T. H., Estrella, N., and Eckhardt, S.: 'SSW to NNE' - North Atlantic Oscillation affects  
556 the progress of seasons across Europe, *Glob. Change Biol.*, 11, 909-918, 2005.

557 Menzel, A., Sparks, T. H., Estrella, N., Koch, E., Aasa, A., Ahas, R., Alm-Kübler, K., Bissolli, P., Braslavská,  
558 O., Briede, A., Chmielewski, F. M., Crepinsek, Z., Curnel, Y., Dahl, Å., Defila, C., Donnelly, A., Filella, Y.,

559 Jatczak, K., Måge, F., Mestre, A., Nordli, Ø., Peñuelas, J., Pirinen, P., Remišová, V., Scheifinger, H., Striz,  
560 M., Susnik, A., Van Vliet, A. J. H., Wielgolaski, F. E., Zach, S., and Zust, A.: European phenological  
561 response to climate change matches the warming pattern, *Glob. Change Biol.*, 12, 1969-1976, 2006.

562 Morisette, J. T., Richardson, A. D., Knapp, A. K., Fisher, J. I., Graham, E. A., Abatzoglou, J., Wilson, B. E.,  
563 Breshears, D. D., Henebry, G. M., Hanes, J. M., and Liang, L.: Tracking the rhythm of the seasons in the  
564 face of global change: phenological research in the 21st century, *Frontiers in Ecology and the*  
565 *Environment*, 7, 253-260, 2008.

566 Müller, R. and Trentmann, J.: CM SAF Meteosat Surface Radiation Daylight Data Set 1.0 - Monthly  
567 Means / Daily Means . Satellite Application Facility on Climate Monitoring, doi:  
568 10.5676/EUM\_SAF\_CM/DAL\_MVIRI\_SEVIRI/V001, 2013. 2013.

569 Myneni, R. B., Keeling, C. D., Tucker, C. J., Asrar, G., and Nemani, R. R.: Increased plant growth in the  
570 northern high latitudes from 1981 to 1991, *Nature*, 386, 698-702, 1997.

571 Pau, S., Wolkovich, E. M., Cook, B. I., Davies, T. J., Kraft, N. J. B., Bolmgren, K., Betancourt, J. L., and  
572 Cleland, E. E.: Predicting phenology by integrating ecology, evolution and climate science, *Glob.*  
573 *Change Biol.*, 17, 3633-3643, 2011.

574 Peñuelas, J.: Phenology feedbacks on climate change, *Science*, 324, 887-888, 2009.

575 Peñuelas, J. and Filella, I.: Phenology: Responses to a warming world, *Science*, 294, 793-795, 2001.

576 Posselt, R., Mueller, R. W., Stöckli, R., and Trentmann, J.: Remote sensing of solar surface radiation for  
577 climate monitoring — the CM-SAF retrieval in international comparison, *Remote Sens. Environ.*, 118,  
578 186-198, 2012.

579 Posselt, R., Müller, R., Stöckli, R., and Trentmann, J.: CM SAF Surface Radiation MVIRI Data Set 1.0 -  
580 Monthly Means / Daily Means / Hourly Means, Satellite Application Facility on Climate Monitoring,  
581 doi: 10.5676/EUM\_SAF\_CM/RAD\_MVIRI/V001, 2011. 2011.

582 Post, E. and Stenseth, N. C.: Climatic variability, plant phenology, and northern ungulates, *Ecology*, 80,  
583 1322-1339, 1999.

584 Potter, C., Tan, P. N., Steinbach, M., Klooster, S., Kumar, V., Myneni, R., and Genovese, V.: Major  
585 disturbance events in terrestrial ecosystems detected using global satellite data sets, *Glob. Change*  
586 *Biol.*, 9, 1005-1021, 2003.

587 Rafferty, N. E., CaraDonna, P. J., Burkle, L. A., Iler, A. M., and Bronstein, J. L.: Phenological overlap of  
588 interacting species in a changing climate: an assessment of available approaches, *Ecology and*  
589 *Evolution*, 3, 3183-3193, 2013.

590 Rodriguez-Galiano, V., Dash, J., and Atkinson, P. M.: Inter-comparison of satellite sensor land surface  
591 phenology and ground phenology in Europe, *Geophys. Res. Lett.*, 42, 2253-2260, 2015a.

592 Rodriguez-Galiano, V., Sanchez-Castillo, M., Chica-Olmo, M., and Chica-Rivas, M.: Machine learning  
593 predictive models for mineral prospectivity: An evaluation of neural networks, random forest,  
594 regression trees and support vector machines, *Ore Geology Reviews*, 71, 804-818, 2015b.

595 Rodriguez-Galiano, V. F., Chica-Olmo, M., and Chica-Rivas, M.: Predictive modelling of gold potential  
596 with the integration of multisource information based on random forest: a case study on the  
597 Rodalquilar area, Southern Spain, *International Journal of Geographical Information Science*, 28, 1336-  
598 1354, 2014.

599 Rutishauser, T., Luterbacher, J., Defila, C., Frank, D., and Wanner, H.: Swiss spring plant phenology  
600 2007: Extremes, a multi-century perspective, and changes in temperature sensitivity, *Geophys. Res.*  
601 *Lett.*, 35, 2008.

602 Saleska, S. R., Didan, K., Huete, A. R., and Da Rocha, H. R.: Amazon forests green-up during 2005  
603 drought, *Science*, 318, 612, 2007.

604 Schwartz, M. D., Ahas, R., and Aasa, A.: Onset of spring starting earlier across the Northern Hemisphere,  
605 *Glob. Change Biol.*, 12, 343-351, 2006.

606 Snyder, R. L., Spano, D., Cesaraccio, C., and Duce, P.: Determining degree-day thresholds from field  
607 observations, *Int. J. Biometeorol.*, 42, 177-182, 1999.

608 Stöckli, R., Rutishauser, T., Baker, I., Liniger, M. A., and Denning, A. S.: A global reanalysis of vegetation  
609 phenology, *Journal of Geophysical Research: Biogeosciences*, 116, G03020, 2011.

610 Stöckli, R., Rutishauser, T., Dragoni, D., O'Keefe, J., Thornton, P. E., Jolly, M., Lu, L., and Denning, A. S.:  
611 Remote sensing data assimilation for a prognostic phenology model, *Journal of Geophysical Research: Biogeosciences*, 113, G04021, 2008.  
612  
613 van Vliet, A. H.: Societal adaptation Options to Changes in Phenology. In: *Phenological Research*,  
614 Hudson, I. L. and Keatley, M. R. (Eds.), Springer Netherlands, Netherlands, 2010.  
615 Vitasse, Y., Delzon, S., Dufrêne, E., Pontailler, J. Y., Louvet, J. M., Kremer, A., and Michalet, R.: Leaf  
616 phenology sensitivity to temperature in European trees: Do within-species populations exhibit similar  
617 responses?, *Agric. For. Meteorol.*, 149, 735-744, 2009.  
618 Yang, X., Mustard, J. F., Tang, J. W., and Xu, H.: Regional-scale phenology modeling based on  
619 meteorological records and remote sensing observations, *Journal of Geophysical Research-Biogeosciences*, 117, 2012.  
620  
621 Yu, R., Schwartz, M. D., Donnelly, A., and Liang, L.: An observation-based progression modeling  
622 approach to spring and autumn deciduous tree phenology, *Int. J. Biometeorol.*, doi: 10.1007/s00484-015-1031-9, 2015.  
623  
624 Zhang, X., Friedl, M. A., Schaaf, C. B., and Strahler, A. H.: Climate controls on vegetation phenological  
625 patterns in northern mid- and high latitudes inferred from MODIS data, *Glob. Change Biol.*, 10, 1133-1145, 2004.  
626  
627 Zhao, M. F., Peng, C. H., Xiang, W. H., Deng, X. W., Tian, D. L., Zhou, X. L., Yu, G. R., He, H. L., and Zhao,  
628 Z. H.: Plant phenological modeling and its application in global climate change research: overview and  
629 future challenges, *Environmental Reviews*, 21, 1-14, 2013.  
630 Zhou, L. M., Tucker, C. J., Kaufmann, R. K., Slayback, D., Shabanov, N. V., and Myneni, R. B.: Variations  
631 in northern vegetation activity inferred from satellite data of vegetation index during 1981 to 1999, *J. Geophys. Res.-Atmos.*, 106, 20069-20083, 2001.  
632

633

634

635 Table 1. Predictors used in the modelling of the ~~temporal variation~~interannual variation in LSP.  
 636 \* predicted over a period of 90 days. \*\* predicted over a period of the 30 and 90 days previous  
 637 to the date of the z-score value.

OG anomalies	EOS anomalies
Averages (M):	
Maximum temperature (TX)**	Maximum temperature (TX)**
Minimum temperature (TN)**	Minimum temperature (TN)**
Average temperature (TG)**	Average temperature (TG)**
Precipitation (PP)**	Precipitation (PP)**
Surface incoming shortwave radiation (SIS)**	Surface incoming shortwave radiation (SIS)**
Surface radiation daylight (DAL)**	Surface radiation daylight (DAL)**
Cumulates (C)	
Growing Degree Days (0° C threshold) (GDD)**	Growing Degree Days (0° C threshold) (GDD)**
Growing Degree Days (5° C threshold) (GDD)**	Growing Degree Days (5° C threshold) (GDD)**
Chilling requirements (CHIL)*	Chilling requirements (CHIL)**
Precipitation (PP)**	Precipitation (PP)**
Surface incoming shortwave radiation (SIS)**	Surface incoming shortwave radiation (SIS)**
Surface radiation daylight (DAL)**	Surface radiation daylight (DAL)**
Date of specific events	
First freeze (FF)*	First freeze (FF)*
Last freeze (LF)*	OG z-score value (OGA) (legacy effect of an advanced or delayed spring)
Period of freeze (PF)*	

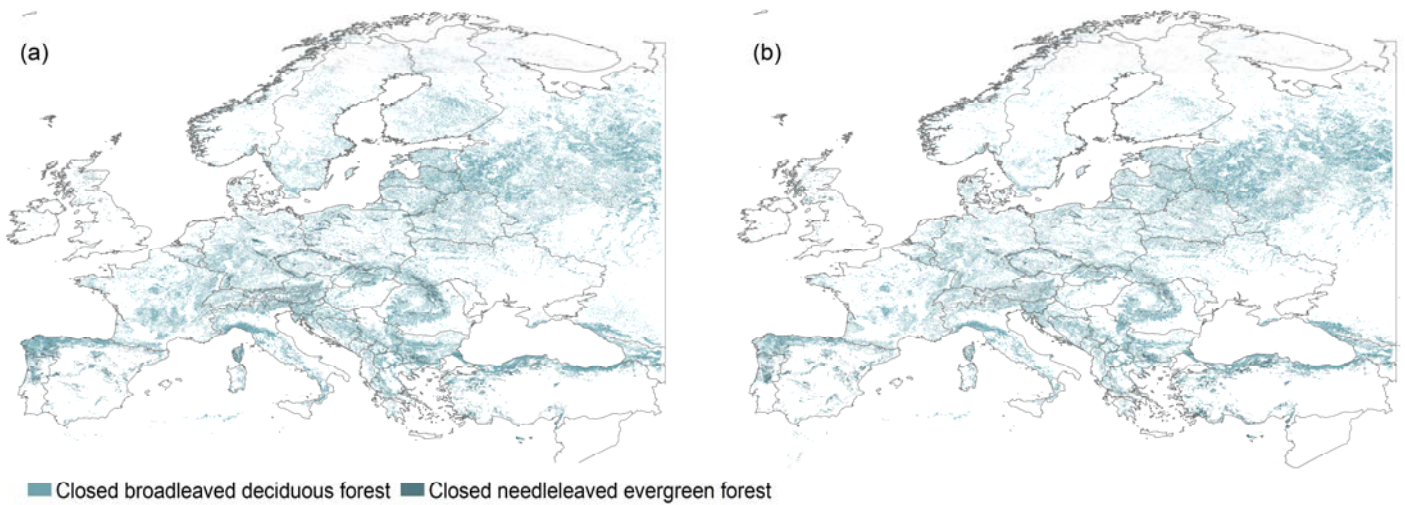
638

1 Table 2. Correlations between the predictors used in the modelling of spring **temporal variation** **interannual variation** in LSP. Significant correlations  
 2 between the anomalies and the predictors are given in bold ( $p < 0.05$ ).

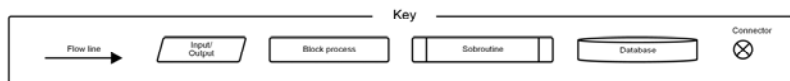
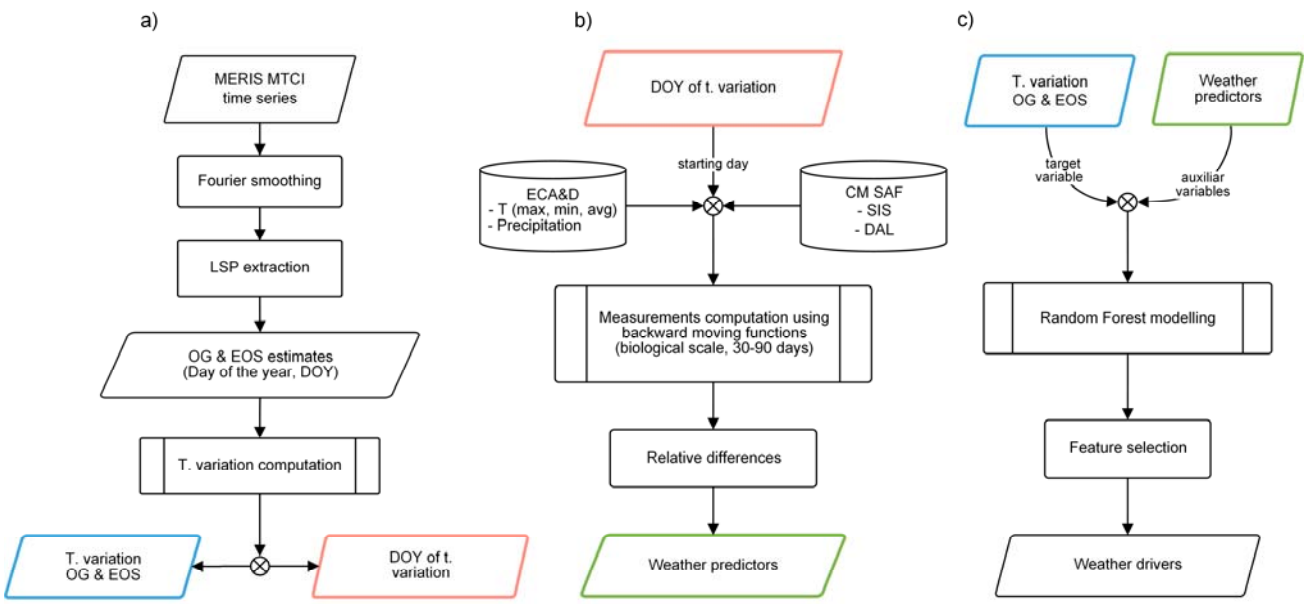
		1	2	3	4	5	6	7	8	9	10	11	12	13	14	15	16	17	18	19	20	21	22	23	24	25	26	27
1	Anom.	<b>1.00</b>	<b>-0.40</b>	<b>-0.43</b>	<b>-0.11</b>	<b>-0.09</b>	<b>-0.12</b>	<b>-0.10</b>	<b>-0.11</b>	<b>-0.10</b>	<b>0.24</b>	-0.03	-0.03	-0.03	<b>-0.14</b>	-0.04	-0.04	<b>-0.33</b>	<b>-0.16</b>	<b>-0.16</b>	-0.04	<b>-0.06</b>	<b>-0.06</b>	<b>-0.45</b>	<b>-0.46</b>	<b>-0.12</b>	<b>-0.31</b>	-0.03
2	GDD090	<b>-0.40</b>	1.00	0.93	0.11	0.14	0.11	0.13	0.11	0.15	-0.64	0.00	-0.01	-0.01	0.23	0.01	0.01	-0.12	-0.06	-0.06	0.04	-0.05	-0.05	0.67	0.64	0.18	-0.11	0.05
3	GDD590	<b>-0.43</b>	0.93	1.00	0.11	0.10	0.11	0.10	0.11	0.11	-0.47	-0.01	-0.01	-0.01	0.16	0.01	0.01	0.03	0.04	0.04	0.06	0.03	0.03	0.74	0.75	0.16	0.03	0.06
4	MTG30	<b>-0.11</b>	0.11	0.11	1.00	0.99	1.00	0.99	1.00	0.98	-0.05	0.89	0.89	0.89	0.20	0.97	0.96	0.02	0.00	0.00	0.31	-0.01	-0.01	0.17	0.15	0.28	0.07	0.31
5	MTG90	<b>-0.09</b>	0.14	0.10	0.99	1.00	0.98	1.00	0.99	1.00	-0.13	0.88	0.88	0.88	0.25	0.96	0.96	-0.03	-0.03	-0.03	0.30	-0.04	-0.04	0.10	0.09	0.29	0.02	0.31
6	MTX30	<b>-0.12</b>	0.11	0.11	1.00	0.98	1.00	0.99	0.99	0.98	-0.04	0.89	0.89	0.88	0.19	0.96	0.96	0.03	0.00	0.00	0.32	-0.01	-0.01	0.18	0.16	0.27	0.08	0.32
7	MTX90	<b>-0.10</b>	0.13	0.10	0.99	1.00	0.99	1.00	0.99	1.00	-0.11	0.89	0.89	0.89	0.23	0.96	0.96	-0.03	-0.03	-0.03	0.30	-0.04	-0.04	0.10	0.09	0.28	0.02	0.31
8	MTN30	<b>-0.11</b>	0.11	0.11	1.00	0.99	0.99	0.99	1.00	0.98	-0.06	0.89	0.89	0.89	0.21	0.96	0.96	0.02	0.01	0.01	0.31	0.00	0.00	0.16	0.14	0.29	0.06	0.31
9	MTN90	<b>-0.10</b>	0.15	0.11	0.98	1.00	0.98	1.00	0.98	1.00	-0.15	0.88	0.88	0.88	0.26	0.96	0.96	-0.04	-0.03	-0.03	0.29	-0.03	-0.03	0.10	0.09	0.30	0.02	0.30
10	CHIL	<b>0.24</b>	-0.64	-0.47	-0.05	-0.13	-0.04	-0.11	-0.06	-0.15	1.00	-0.01	0.00	0.00	-0.25	0.00	0.00	0.28	0.11	0.11	0.03	0.06	0.06	-0.24	-0.26	-0.16	0.26	0.01
11	FF	-0.03	0.00	-0.01	0.89	0.88	0.89	0.89	0.89	0.88	-0.01	1.00	1.00	1.00	-0.01	0.88	0.88	-0.04	-0.05	-0.05	0.00	-0.06	-0.06	0.00	-0.01	-0.01	-0.03	0.00
12	LF	-0.03	-0.01	-0.01	0.89	0.88	0.89	0.89	0.89	0.88	0.00	1.00	1.00	1.00	-0.01	0.88	0.88	-0.04	-0.05	-0.05	0.00	-0.06	-0.06	-0.01	-0.01	-0.01	-0.03	0.00
13	PF	-0.03	-0.01	-0.01	0.89	0.88	0.88	0.89	0.89	0.88	0.00	1.00	1.00	1.00	-0.02	0.88	0.88	-0.04	-0.05	-0.05	0.00	-0.06	-0.06	-0.01	-0.01	-0.03	0.00	
14	CRR90	<b>-0.14</b>	0.23	0.16	0.20	0.25	0.19	0.23	0.21	0.26	-0.25	-0.01	-0.01	-0.02	1.00	0.20	0.20	0.01	0.06	0.06	0.53	0.04	0.04	0.09	0.07	0.77	0.11	0.58
15	MRR30	-0.04	0.01	0.01	0.97	0.96	0.96	0.96	0.96	0.96	0.00	0.88	0.88	0.88	0.20	1.00	1.00	0.00	-0.03	-0.03	0.31	-0.03	-0.03	0.03	0.03	0.26	0.05	0.31
16	MRR90	-0.04	0.01	0.01	0.96	0.96	0.96	0.96	0.96	0.96	0.00	0.88	0.88	0.88	0.20	1.00	1.00	0.00	-0.03	-0.03	0.31	-0.03	-0.03	0.03	0.02	0.26	0.05	0.31
17	CSIS90	<b>-0.33</b>	-0.12	0.03	0.02	-0.03	0.03	-0.03	0.02	-0.04	0.28	-0.04	-0.04	-0.04	0.01	0.00	0.00	1.00	0.80	0.80	0.16	0.57	0.57	0.22	0.22	0.12	0.96	0.15
18	MSIS30	<b>-0.16</b>	-0.06	0.04	0.00	-0.03	0.00	-0.03	0.01	-0.03	0.11	-0.05	-0.05	-0.05	0.06	-0.03	-0.03	0.80	1.00	1.00	0.06	0.90	0.90	0.23	0.24	0.15	0.77	0.06
19	MSIS90	<b>-0.16</b>	-0.06	0.04	0.00	-0.03	0.00	-0.03	0.01	-0.03	0.11	-0.05	-0.05	-0.05	0.06	-0.03	-0.03	0.80	1.00	1.00	0.06	0.90	0.90	0.23	0.24	0.15	0.77	0.06
20	CDAL90	-0.04	0.04	0.06	0.31	0.30	0.32	0.30	0.31	0.29	0.03	0.00	0.00	0.00	0.53	0.31	0.31	0.16	0.06	0.06	1.00	0.05	0.05	0.11	0.10	0.78	0.28	0.99
21	MDAL30	<b>-0.06</b>	-0.05	0.03	-0.01	-0.04	-0.01	-0.04	0.00	-0.03	0.06	-0.06	-0.06	-0.06	0.04	-0.03	-0.03	0.57	0.90	0.90	0.05	1.00	1.00	0.23	0.23	0.13	0.55	0.05
22	MDAL90	<b>-0.06</b>	-0.05	0.03	-0.01	-0.04	-0.01	-0.04	0.00	-0.03	0.06	-0.06	-0.06	-0.06	0.04	-0.03	-0.03	0.57	0.90	0.90	0.05	1.00	1.00	0.23	0.23	0.13	0.55	0.05
23	GDD030	<b>-0.45</b>	0.67	0.74	0.17	0.10	0.18	0.10	0.16	0.10	-0.24	0.00	-0.01	-0.01	0.09	0.03	0.03	0.22	0.23	0.23	0.11	0.23	0.23	1.00	0.97	0.16	0.23	0.11
24	GDD530	<b>-0.46</b>	0.64	0.75	0.15	0.09	0.16	0.09	0.14	0.09	-0.26	-0.01	-0.01	-0.01	0.07	0.03	0.02	0.22	0.24	0.24	0.10	0.23	0.23	0.97	1.00	0.15	0.24	0.10
25	CRR30	<b>-0.12</b>	0.18	0.16	0.28	0.29	0.27	0.28	0.29	0.30	-0.16	-0.01	-0.01	-0.01	0.77	0.26	0.26	0.12	0.15	0.15	0.78	0.13	0.13	0.16	0.15	1.00	0.18	0.79
26	CSIS30	<b>-0.31</b>	-0.11	0.03	0.07	0.02	0.08	0.02	0.06	0.02	0.26	-0.03	-0.03	-0.03	0.11	0.05	0.05	0.96	0.77	0.77	0.28	0.55	0.55	0.23	0.24	0.18	1.00	0.28
27	CDAL30	-0.03	0.05	0.06	0.31	0.31	0.32	0.31	0.31	0.30	0.01	0.00	0.00	0.00	0.58	0.31	0.31	0.15	0.06	0.06	0.99	0.05	0.05	0.11	0.10	0.79	0.28	1.00

1 Table 3. Correlations between the predictors used in the modelling of autumn ~~temporal variation~~interannual variation in LSP. Significant  
 2 correlations between the anomalies and the predictors are given in bold ( $p < 0.05$ ).

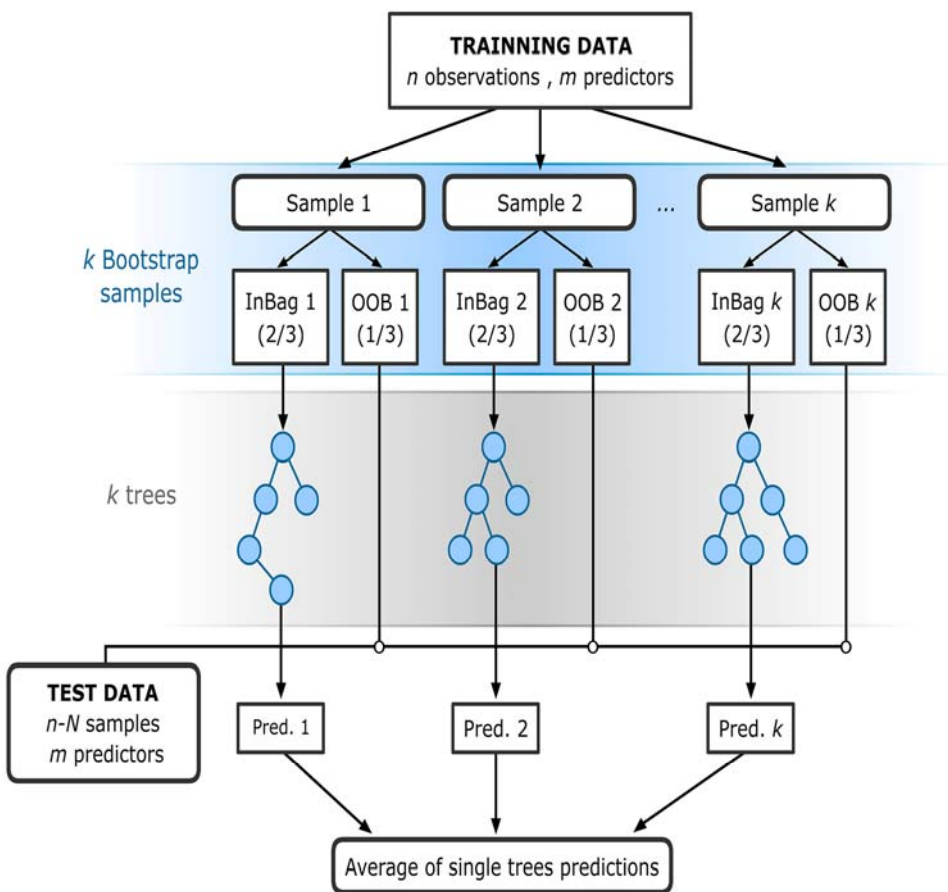
		1	2	3	4	5	6	7	8	9	10	11	12	13	14	15	16	17	18	19	20	21	22	23	24	25	26	27
1	Anom.	1	<b>0.10</b>	<b>0.31</b>	<b>0.34</b>	<b>0.33</b>	<b>0.36</b>	<b>0.28</b>	<b>0.30</b>	<b>0.28</b>	<b>0.27</b>	<b>0.26</b>	<b>0.34</b>	0.01	-0.03	<b>0.34</b>	<b>0.07</b>	<b>0.07</b>	0.04	<b>-0.05</b>	-0.05	-0.05	0.00	-0.01	<b>-0.08</b>	<b>-0.08</b>	<b>-0.09</b>	<b>-0.15</b>
2	OGA	0.10	1.00	0.06	0.08	0.14	0.16	0.05	0.15	0.02	0.07	0.05	0.19	-0.02	-0.04	0.01	0.02	-0.05	-0.07	0.06	-0.02	-0.02	-0.10	-0.11	0.01	0.01	-0.06	-0.10
3	GDD030	0.31	0.06	1.00	0.97	0.54	0.58	0.94	0.53	0.88	0.42	0.87	0.62	-0.54	-0.52	0.25	0.09	0.10	0.11	0.03	-0.09	-0.09	-0.01	0.01	-0.22	-0.22	-0.11	-0.22
4	GDD530	0.34	0.08	0.97	1.00	0.53	0.60	0.86	0.49	0.80	0.37	0.80	0.59	-0.41	-0.40	0.24	0.11	0.11	0.10	0.07	-0.10	-0.10	-0.03	-0.01	-0.23	-0.23	-0.15	-0.25
5	GDD090	0.33	0.14	0.54	0.53	1.00	0.98	0.49	0.95	0.54	0.90	0.36	0.85	-0.14	-0.24	0.12	0.05	0.13	0.09	-0.15	-0.07	-0.07	0.04	-0.05	-0.14	-0.14	0.08	-0.14
6	GDD590	0.36	0.16	0.58	0.60	0.98	1.00	0.49	0.92	0.54	0.85	0.37	0.84	-0.10	-0.20	0.14	0.07	0.13	0.09	-0.11	-0.07	-0.07	0.02	-0.06	-0.14	-0.14	0.04	-0.19
7	MTG30	0.28	0.05	0.94	0.86	0.49	0.49	1.00	0.56	0.93	0.44	0.94	0.63	-0.71	-0.66	0.24	0.04	0.10	0.09	-0.01	-0.02	-0.02	0.02	0.05	-0.13	-0.13	-0.09	-0.17
8	MTG90	0.30	0.15	0.53	0.49	0.95	0.92	0.56	1.00	0.61	0.93	0.43	0.89	-0.28	-0.36	0.12	-0.01	0.13	0.09	-0.18	0.02	0.02	0.07	-0.01	-0.03	-0.03	0.09	-0.11
9	MTX30	0.28	0.02	0.88	0.80	0.54	0.54	0.93	0.61	1.00	0.58	0.78	0.60	-0.58	-0.54	0.20	-0.09	0.12	0.07	-0.09	0.03	0.03	0.23	0.14	-0.09	-0.09	0.17	-0.06
10	MTX90	0.27	0.07	0.42	0.37	0.90	0.85	0.44	0.93	0.58	1.00	0.28	0.73	-0.16	-0.24	0.09	-0.05	0.13	0.05	-0.31	0.02	0.02	0.17	0.07	-0.03	-0.03	0.23	0.07
11	MTN30	0.26	0.05	0.87	0.80	0.36	0.37	0.94	0.43	0.78	0.28	1.00	0.61	-0.76	-0.70	0.26	0.16	0.08	0.09	0.08	-0.06	-0.06	-0.17	-0.04	-0.14	-0.14	-0.30	-0.24
12	MTN90	0.34	0.19	0.62	0.59	0.85	0.84	0.63	0.89	0.60	0.73	0.61	1.00	-0.39	-0.48	0.19	0.12	0.13	0.12	0.04	-0.02	-0.02	-0.07	-0.12	-0.06	-0.06	-0.08	-0.31
13	CHIL30	0.01	-0.02	-0.54	-0.41	-0.14	-0.10	-0.71	-0.28	-0.58	-0.16	-0.76	-0.39	1.00	0.91	-0.08	-0.05	0.00	0.01	-0.05	-0.05	-0.05	0.09	-0.01	-0.01	0.17	0.10	
14	CHIL90	-0.03	-0.04	-0.52	-0.40	-0.24	-0.20	-0.66	-0.36	-0.54	-0.24	-0.70	-0.48	0.91	1.00	-0.09	-0.04	0.00	0.01	-0.05	-0.08	-0.08	0.08	0.01	-0.04	-0.04	0.16	0.15
15	FF	<b>0.34</b>	0.01	0.25	0.24	0.12	0.14	0.24	0.12	0.20	0.09	0.26	0.19	-0.08	-0.09	1.00	-0.10	0.05	0.04	-0.08	0.01	0.01	0.01	0.07	-0.05	-0.05	-0.08	-0.04
16	CRR30	<b>0.07</b>	0.02	0.09	0.11	0.05	0.07	0.04	-0.01	-0.09	-0.05	0.16	0.12	-0.05	-0.04	-0.10	1.00	0.12	0.04	0.51	-0.17	-0.17	-0.42	-0.25	-0.12	-0.12	-0.46	-0.25
17	MRR30	<b>0.07</b>	-0.05	0.10	0.11	0.13	0.13	0.10	0.13	0.12	0.13	0.08	0.13	0.00	0.00	0.05	0.12	1.00	0.47	0.08	-0.03	-0.03	-0.02	-0.03	-0.03	-0.03	-0.02	-0.04
18	MRR90	0.04	-0.07	0.11	0.10	0.09	0.09	0.09	0.09	0.07	0.05	0.09	0.12	0.01	0.01	0.04	0.04	0.47	1.00	0.06	-0.01	-0.01	-0.02	-0.04	-0.02	-0.02	-0.02	-0.08
19	CRR90	<b>-0.05</b>	0.06	0.03	0.07	-0.15	-0.11	-0.01	-0.18	-0.09	-0.31	0.08	0.04	-0.05	-0.05	-0.08	0.51	0.08	0.06	1.00	-0.04	-0.05	-0.14	-0.18	-0.05	-0.05	-0.20	-0.39
20	MSIS30	<b>-0.05</b>	-0.02	-0.09	-0.10	-0.07	-0.07	-0.02	0.02	0.03	0.02	-0.06	-0.02	-0.05	-0.08	0.01	-0.17	-0.03	-0.01	-0.04	1.00	1.00	0.56	0.66	0.88	0.88	0.05	-0.04
21	MSIS90	<b>-0.05</b>	-0.02	-0.09	-0.10	-0.07	-0.07	-0.02	0.02	0.03	0.02	-0.06	-0.02	-0.05	-0.08	0.01	-0.17	-0.03	-0.01	-0.05	1.00	1.00	0.55	0.66	0.88	0.88	0.05	-0.04
22	CSIS30	0.00	-0.10	-0.01	-0.03	0.04	0.02	0.02	0.07	0.23	0.17	-0.17	-0.07	0.09	0.08	0.01	-0.42	-0.02	-0.02	-0.14	0.56	0.55	1.00	0.80	0.30	0.30	0.66	0.28
23	CSIS90	-0.01	-0.11	0.01	-0.01	-0.05	-0.06	0.05	-0.01	0.14	0.07	-0.04	-0.12	-0.01	0.01	0.07	-0.25	-0.03	-0.04	-0.18	0.66	0.66	0.80	1.00	0.31	0.31	0.18	0.40
24	MDAL30	<b>-0.08</b>	0.01	-0.22	-0.23	-0.14	-0.14	-0.13	-0.03	-0.09	-0.03	-0.14	-0.06	-0.01	-0.04	-0.05	-0.12	-0.03	-0.02	-0.05	0.88	0.88	0.30	0.31	1.00	1.00	0.05	-0.05
25	MDAL90	<b>-0.08</b>	0.01	-0.22	-0.23	-0.14	-0.14	-0.13	-0.03	-0.09	-0.03	-0.14	-0.06	-0.01	-0.04	-0.05	-0.12	-0.03	-0.02	-0.05	0.88	0.88	0.30	0.31	1.00	1.00	0.05	-0.05
26	CDAL30	<b>-0.09</b>	-0.06	-0.11	-0.15	0.08	0.04	-0.09	0.09	0.17	0.23	-0.30	-0.08	0.17	0.16	-0.08	-0.46	-0.02	-0.02	-0.20	0.05	0.05	0.66	0.18	0.05	0.05	1.00	0.41
27	CDAL90	<b>-0.15</b>	-0.10	-0.22	-0.25	-0.14	-0.19	-0.17	-0.11	-0.06	0.07	-0.24	-0.31	0.10	0.15	-0.04	-0.25	-0.04	-0.08	-0.39	-0.04	-0.04	0.28	0.40	-0.05	-0.05	0.41	1.00



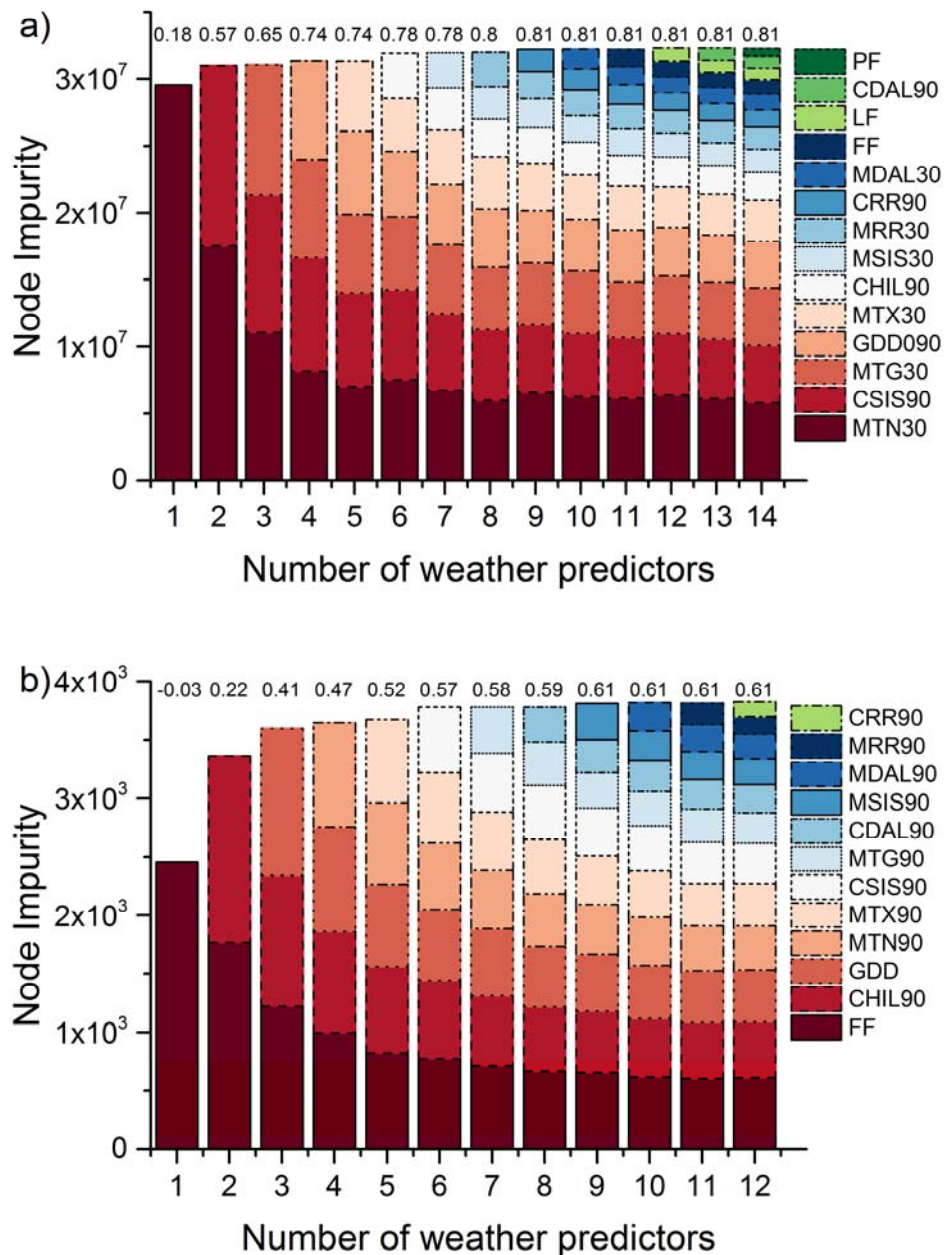
2 Figure 1. Spatial distribution of GlobCover broadleaved deciduous forest and needleleaved  
3 evergreen forest in 2005 (a) and 2009 (b).



2 Figure 2. Flow-chart illustrating the methodology. A) Phenology extraction and **temporal**  
3 **variation****interannual variation** in LSP computation. B) Computation of weather predictors. C)  
4 Modelling of **temporal variation****interannual variation** in phenology.

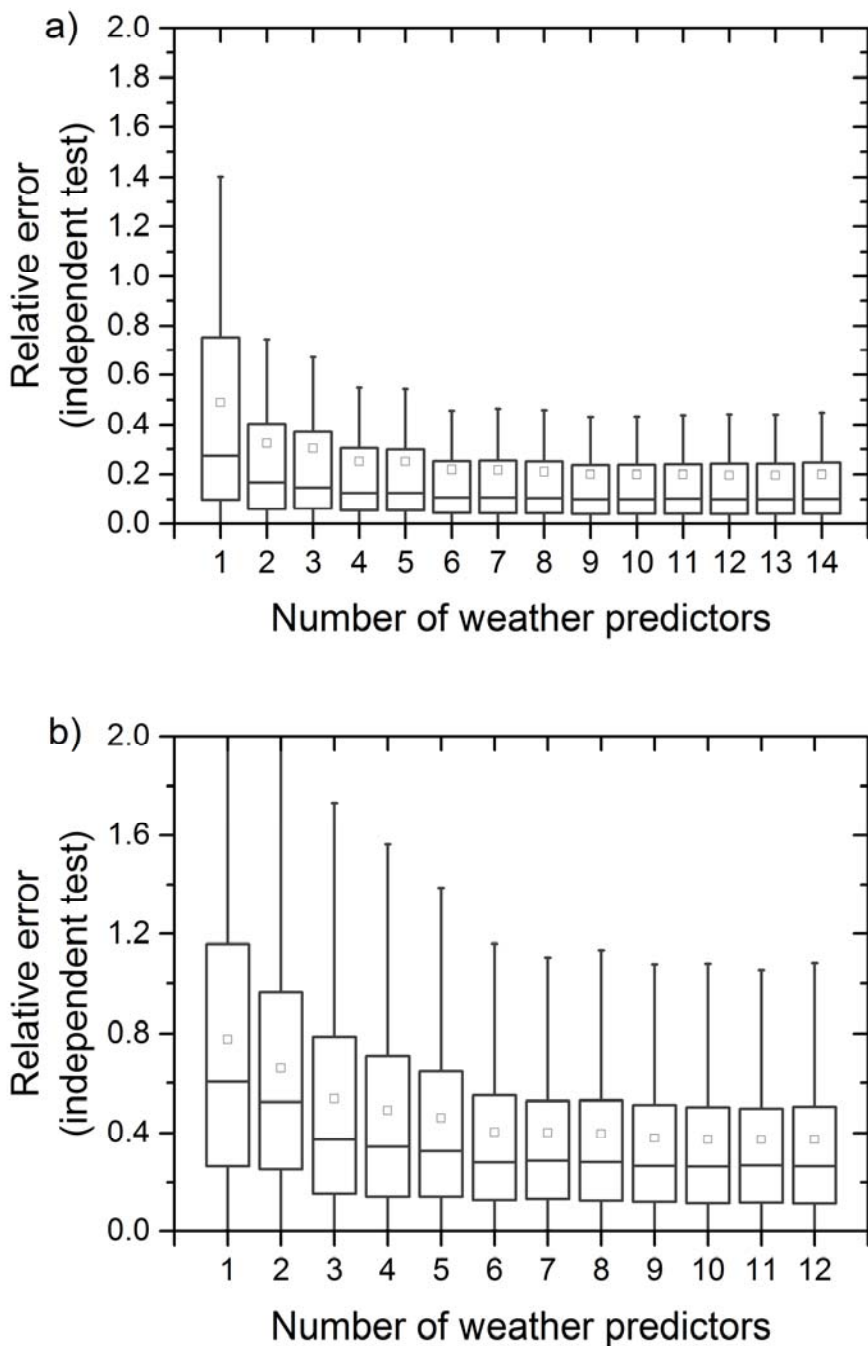


1  
 2 Figure 3. The flowchart of Random Forest for regression (adapted from Rodriguez-Galiano et  
 3 al. 2015b). The RF method receives a subset of input vectors (n), made up of one phenology z-  
 4 score value and the values of the corresponding weather predictors for a given location and  
 5 year. RF builds a number K of regression trees making them grow from different training data  
 6 subsets, resampling randomly the original dataset with replacement. Hence, most data will be  
 7 used multiple times in different models. On the other hand, when the RF makes a tree grow, it  
 8 uses the best predictor within a subset of predictors (m) which has been selected randomly from  
 9 the overall set of input predictors. These especial characteristics of RF confer a greater  
 10 prediction stability and accuracy and, at the same time, avoid the correlation of the different  
 11 RTs, increasing the diversity of patterns that can be learnt from data. The multiple predictions  
 12 of all k RTs for a given vector used as training are then averaged to obtain a unique estimation  
 13 of the phenology z-score value.



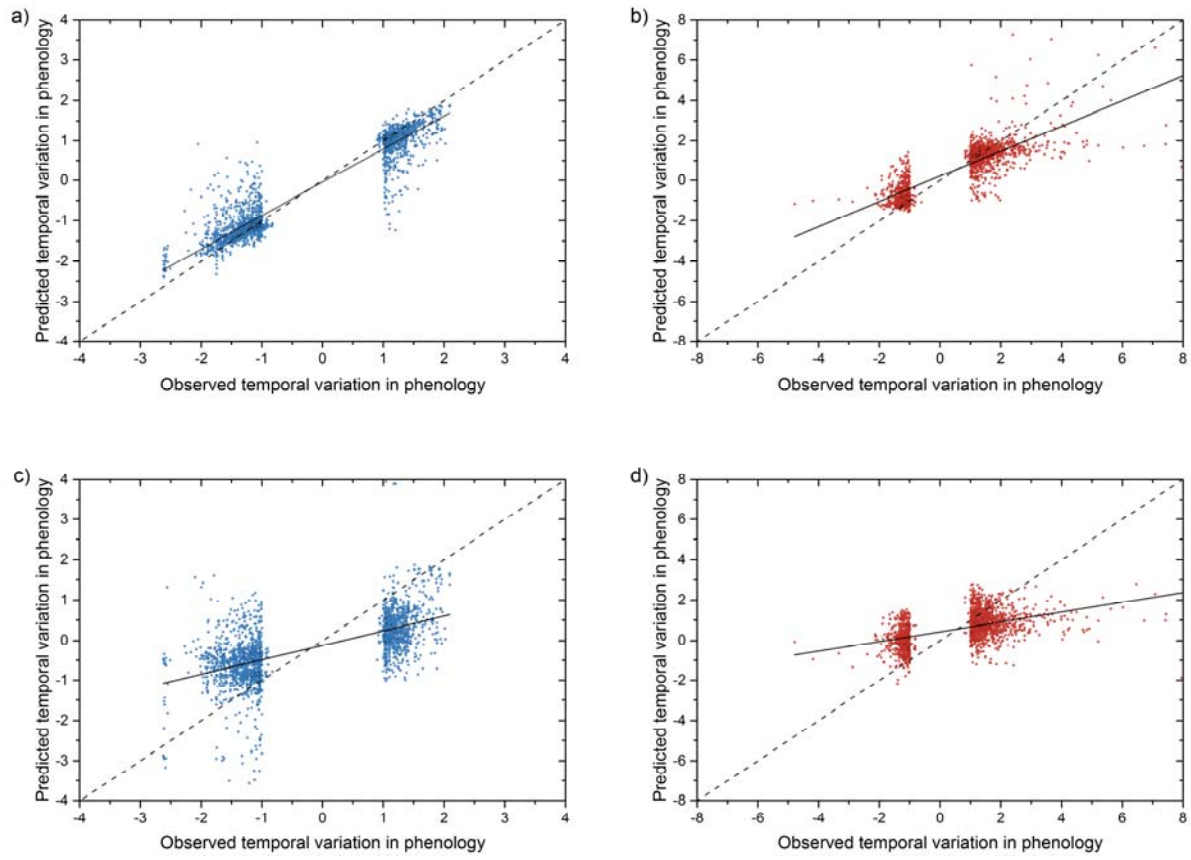
1  
2 Figure 43. Relative importance of each independent variable in predicting phenology ~~temporal variation~~  
3 ~~interannual variation in Europe~~. -Different models derived from the feature selection  
4 approach are represented in each column. Numbers given over each column represent the  
5 coefficient determination of each model. Plots at the top and bottom represent the spring (a)  
6 and autumn ~~temporal variation~~  
7 ~~interannual variation~~ in LSP (b), respectively. The names of  
8 predictors follows the notation: Prefix M and C represent the mean and cumulated functions;  
9 TX, TN and TG: maximum, minimum and average temperature, respectively; PP: precipitation;  
SIS: surface incoming shortwave radiation; DAL: surface radiation daylight; GDD: growing

1 degree days; CHIL: chilling requirements; FF, LF and PF: first, last and period of freeze,  
2 respectively.



1  
2 Figure 54. Relative error of the models fitted as a result of the feature selection approach.  
3 Median (interior horizontal line), mean (interior square), 1% and 99% quantiles (edge of boxes),  
4 range (extremes). Relative errors were calculated for the prediction of 1,974 and 1,576  
5 independent observations for spring (a) and autumn (b), respectively. See previous figure for  
6 the weather predictor variables in the models, as shown in the x-axis.

7



1      Figure 65. Scatterplots between observed anomalies in LSP and the predictions calculated  
 2 using a selection of weather predictors (see Figure 2 and Figure 3). Plots for spring phenology  
 3 are shown on the left panel (blue; a, c) and autumn on the right (red; b, d). Random Forest  
 4 predictions are given in the upper panel (a, b) and those of the linear regression in the bottom  
 5 (c, d) panel. The dashed lines represent an exact 1:1 relationship (expected fitting), the solid  
 6 lines show a linear regression of these data. The explained variances (percentage  $R^2$ ) and RMSE  
 7 values are 90% and 0.43 (spring Random Forest model), 68% and 0.92 (autumn Random Forest  
 8 model), 39% and 1.04 (spring Linear model) and 25% 1.40 (autumn linear model).  
 9